AD-A060 383 WYOMING UNIV LARAMIE DEPT OF PHYSICS AND ASTRONOMY F/G 7/4
UNIVERSITY OF WYOMING/LENINGRAD STATE UNIVERSITY COOPERATIVE ST--ETC(U)
JUL 78 J M ROSEN, D J HOFMANN DOT-FAA76WA-3782
UNCLASSIFIED FAA-AEQ-78-22 NL

1 OF 2
AD
A060 383

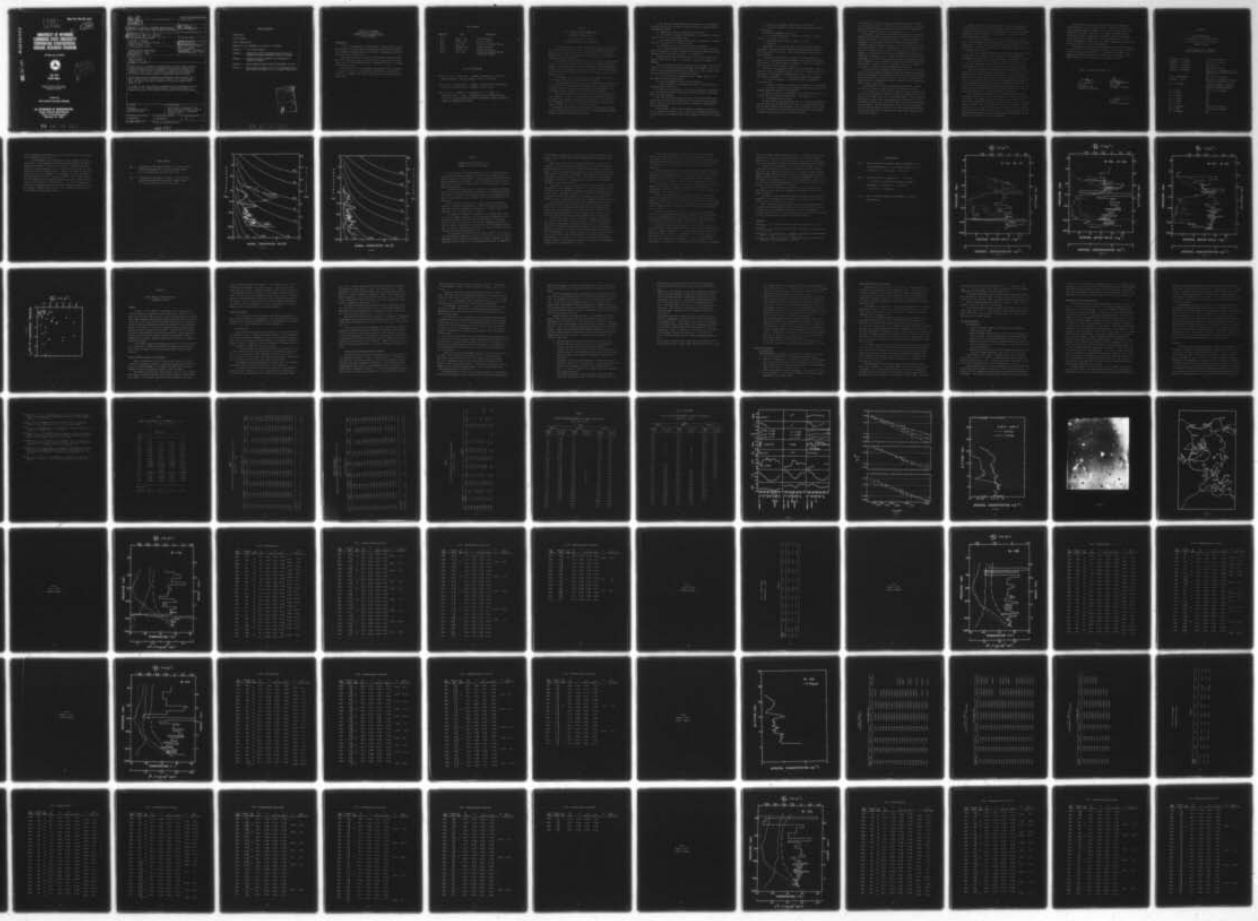

LEVEL II

Report No. FAA- AEQ -78-22

12

UNIVERSITY OF WYOMING
LENINGRAD STATE UNIVERSITY
COOPERATIVE STRATOSPHERIC
AEROSOL RESEARCH PROGRAM

J.M. Rosen and D.J. Hofmann

July 1978
Interim Report

Prepared for

HIGH ALTITUDE POLLUTION PROGRAM

U.S. DEPARTMENT OF TRANSPORTATION
FEDERAL AVIATION ADMINISTRATION
Office of Environmental Quality
Washington, D.C. 20591

Technical Report Documentation Page

1. Report No.	2. Government Accession No.	3. Recipient's Catalog No.
FAA-AEQ-78-22		

4. Title and Subtitle

UNIVERSITY OF WYOMING / LENINGRAD STATE UNIVERSITY COOPERATIVE STRATOSPHERIC AEROSOL RESEARCH PROGRAM

5. Report Date: July 1978

6. Performing Organization Code

7. Author(s): James M. Rosen and David J. Hofmann

8. Performing Organization Report No.

9. Performing Organization Name and Address

University of Wyoming
Department of Physics and Astronomy
Laramie, Wyoming 82071

407 537

10. Work Unit No. (TRAIS)

11. Contract or Grant No.: DOT-FAA76WA-3782

13. Type of Report and Period Covered: Interim Report, March 1976 - July 1978

12. Sponsoring Agency Name and Address

Federal Aviation Administration
800 Independence Avenue, S.W.
Washington, D.C. 20591

14. Sponsoring Agency Code

15. Supplementary Notes

12) 103 p.

16. Abstract

In 1974, the U.S. Department of Transportation's Climatic Impact Assessment Program initiated a study of stratospheric aerosols which consisted of a cooperative program between the University of Wyoming and Leningrad State University in the U.S.S.R. Since 1975, the program has been continued by the Federal Aviation Administration, High Altitude Pollution Program.

This program resulted in cooperative stratospheric balloon flights from a Soviet balloon launch facility at Rylsk, in the U.S.S.R., during August of 1975, and from the University of Wyoming's facility in Laramie, during August of 1976.

In November of 1977, the principal investigators met in Leningrad to discuss the results of the comparative measurements. This meeting resulted in a lengthy joint report, which serves as the main body of this interim report.

17. Key Words	18. Distribution Statement
Aerosols Stratospheric aerosols Radiation transfer	This document is available to the public through the National Technical Information Service, Springfield, Virginia 22161

19. Security Classif. (of this report)	20. Security Classif. (of this page)	21. No. of Pages	22. Price
UNCLASSIFIED	UNCLASSIFIED	103	

Form DOT F 1700.7 (8-72) Reproduction of completed page authorized

407 537

TABLE OF CONTENTS

UNIVERSITY OF WYOMING
LENINGRAD STATE UNIVERSITY
COOPERATIVE STRATOSPHERIC AEROSOL
RESEARCH PROGRAM

INTRODUCTION

In 1974, the Department of Transportation's Climatic Impact Assessment Program initiated a study of stratospheric aerosol which consisted of a cooperative program between the University of Wyoming and Leningrad State University in the U.S.S.R.

This program resulted in cooperative stratospheric balloon flights from a Soviet balloon launch facility at Rylsk, in the U.S.S.R., during August of 1975, and from the University of Wyoming's facility, in Laramie, during August of 1976.

In November of 1977, the principal investigators went to Leningrad, to discuss the results of the comparative measurements. This meeting resulted in a lengthy joint report, which serves as the main body of this final report.

LIST OF REPORTS

Report No.	Date	Description
WL-1	August, 1975	Rylsk Expedition
WL-2	October, 1975	Rylsk Data Report
WL-3	June, 1976	Protocol of Leningrad Meeting
WL-4	September, 1976	Laramie Expedition
WL-5	January, 1977	Laramie Data Report
WL-6	July, 1978	Protocol of Leningrad Meeting and USSR Data Report

LIST OF PUBLICATIONS

Rosen, J. M., N. T. Kjome and D. J. Hofmann, "Cooperative U.S.-U.S.S.R. Balloon Flights," Bull. Am. Meteorol. Soc. 57, 225 (1976).

Rosen, J. M. N. T. Kjome and D. J. Hofmann, "Cooperative Research Between the U.S.A. and the U.S.S.R.," WMO Bull. 25, 236 (1976).

Rosen, J. M., D. J. Hofmann, K. Ya. Kondratyev, V. A. Ivanov, A. G. Laktionov, and L. S. Ivlev, "Comparison of Results Obtained during the U.S.S.R.-U.S.A. Cooperative Aerosol Measurement Program in Laramie," submitted to WMO Bulletin, (1978).

PROTOCOL

of the meeting of the USA/USSR experts
on the results of the
stratospheric aerosol studies

20-26 November, 1977, Leningrad

Voeikov Main Geophysical Observatory

For implementation of the USA/USSR bilateral agreement on cooperation in the Protection of the Environment, several joint working groups have been set up consisting of scientists from both countries. The task of Working Group VIII was to investigate various aspects of the influence of environmental change on climate.

In accordance with the agreement on the joint studies program reached at the first meeting of WGVIII ("The Influence of Environmental Change on Climate"), in Leningrad, June 10-21, 1974, combined studies of atmospheric aerosol (mainly stratospheric aerosol) and its effect on radiation transfer were carried out in the Rylsk area from July 27 to August 11, 1975, at the CAO balloon base.

The experiment was carried out within the framework of Project II, on the "Joint Study of Air Pollution Impact on Climate."

The Main Geophysical Observatory, the Central Aerological Observatory and the University of Leningrad (on the Soviet side) and the University of Wyoming (on the American side) participated in the experiment. The experiment involved balloon, aircraft and surface measurements.

Three balloon launches of the Soviet and American instruments were made on August 1, 3 and 5. The USSR balloon-borne equipment consisted of a) impactor for continuous sampling with a moving plate, b) filter trap. The US equipment consisted of a photoelectric counter for particles in range of radius $\geq$ 0.15 μm and r $\geq$ 0.25 μm (dustsonde).

The Soviet scientists launched aerological and actinometric radiosondes to obtain data on the vertical profile of meteorological parameters and data concerning longwave radiation fluxes.

At the same time, aerosol-radiation measurements in the troposphere were made from on board the MGO IL-18 flying laboratory equipped with the following instruments:

a) impactor for continuous sampling and filter traps;

b) spectrometers for spectral measurements of hemispherical radiation fluxes in the 0.4-1 μm wavelength range;

c) instruments for integrated measurements of hemispherical radiation fluxes in the ranges of 0.3-3 μm and 3-30 μm;

d) instruments for measuring meteorological parameters.

A set of surface observations was carried out which involved measurements of atmospheric spectral transparency and solar radiation observations. The experiment in Rylsk was successful. (See Appendix 4).

At the second meeting of Working Group VIII, held in Princeton, New Jersey, October 20-31, 1976, it was agreed to continue the cooperative program.

The Soviet-American meeting on discussion and assessment of the results of the 1975 joint balloon-launched measurements of atmospheric aerosol was held in the Main Geophysical Observatory on May 18-25, 1976. Special attention was paid to the analysis of the following data:

a) vertical profile of atmospheric aerosol (number density, size distribution, chemical composition);

b) spectral shortwave radiation flux divergences;

c) optical properties of atmospheric thickness, and the surface atmospheric layer, in particular.

The problems of the dynamics of origin and development of atmospheric processes and other phenomena affecting the radiative regime in the atmosphere were also discussed.

The results obtained in Rylsk have made it possible to specify the program of the second joint experiment (in the region of Laramie, Wyoming, USA) in August of 1976,which involved Soviet and American balloon-borne aerosol measurements.

Three launches of the Soviet and American instruments were made on July 31, August 4 and August 6, 1976. The Soviet instrumentation developed at the University of Leningrad and the Main Geophysical Observatory consisted of:

a) impactor for continuous sampling with a moving plate;

b) filter which sampled the aerosol within three height-intervals in the atmosphere.

The American equipment consisted of:

a) a two-channel photoelectric counter of particles in range of radius $\geq$ 0.15 μm and r $\geq$ 0.25 μm;

b) condensation-nuclei counter (radius $\geq$ 0.01 μm);

c) ozonesonde.

Additionally, five nocturnal launches of the Soviet actinometric radiosondes were made to measure downward and upward radiation fluxes in the 4-40 μm range of wavelength. They were made before balloon-borne aerosol sampling.

In addition to this program, scientists of NOAA carried out two launches for air-sampling in the stratosphere. The samples obtained were then analyzed in the NOAA Laboratory in Boulder, Colorado, for content of NO_2; $CFCl_3$ (Freon 11); and CF_2Cl_2 (Freon 12).

According to the agreement reached at the Third Meeting of Working Group VIII, held in Leningrad, October 4-14, 1977, a meeting was held in the Main Geophysical Observatory on November 20-26, 1977. (For a list of participants see Appendix 1). The following problems were discussed.

a) the vertical profiles of atmospheric aerosol, condensation nuclei and ozone;

b) results of actinometric and upper air soundings of the atmosphere;

c) the effect of meteorological conditions, aerosol and ozone on the longwave radiation transfer in the atmosphere;

d) possible reasons for differences in the aerosol vertical profiles from the data of the impactor and dustsonde; (see Appendix 2);

e) stratospheric aerosol nature.

The data obtained have enlarged the data set on aerosol distribution over the territories of the USSR and USA, and are of considerable interest for the study of origin and development of the stratospheric aerosol layer at the 15-22 km level, for calculation of the heat field in the atmosphere and comparison with the data of actinometric sounding.

The similarity of radiative properties of the aerosol layer and clouds should be noted, as well as the fact that the change of the sign of the rate of radiative change of temperature may be an indirect indication of aerosol in actinometric samples. (See Appendix 3).

Manuscripts, concerning the preliminary results of the cooperative program, were published in Gydrometeoizdat ("Influence of Aerosols on the Radiation Properties of the Atmosphere: Results of the Soviet-American Experiment"), the Bulletin of the World Meteorological Organization ("USSR-USA Cooperative Research Program"), and in the Bulletin of the American Meteorological Society, ("Cooperative U.S.-U.S.S.R. Balloon Flights"), the latter including a cover picture of a balloon launch at Rylsk. In addition, a joint manuscript, on the aerosol comparison at Laramie, presented here as Appendix 2, was submitted for publication to the Bulletin of the WMO, and a joint article concerning the Rylsk experiment, presented here as Appendix 4, will be submitted to the Soviet journal, Meteorology and Hydrology. Appendix 3, on the actinometric results, will appear as an article in "Reports of the Main Geophysical Observatory."

The results of the accomplished experiments testify to the fruitfulness of the Soviet-American cooperation within the program of the Aerosol-Radiation Experiment. The results obtained, however, should be considered only as the first step in the cooperation, since they are promising for future profound and comprehensive studies of mutual interest using complementary means of investigation.

The continuation of this cooperation of aerosol study is highly desirable for a number of reasons, some of them indicated earlier.

The joint group of experts wish to indicate, having in mind that the realization of the proposed cooperative effort will depend on the availability of U.S. funds in the case of dustsonde flights, to the co-chairmen of Working Group VIII, that a unique opportunity for extensive study of stratospheric aerosol will exist in late 1978, when the satellite Nimbus G will be launched. Aerosol measurements by solar extinction techniques will be conducted from the satellite by the NASA Langley Research Center. The satellite orbit will be such that only a small band of American territory will be observed.

Extensive territory in the Soviet Union suggests the opportunity of comparative studies at or near the geographical satellite occultation points within the Soviet Union. Such measurements, using well established techniques, would be valuable as "ground truth" for the remote sensing aerosol measurement technique.

It will be easier for the American side to participate in such an effort, with dustsondes that could be loaned to the Soviet side during the experiment, if a group of Soviet scientists traveled to the U.S.A. and learned how to operate such equipment. The University of Wyoming is willing to cooperate in this effort.

If the co-chairmen of Working Group VIII find our suggestions of value, we hope they would recommend to the Joint American Soviet Committee on Environmental Protection that they include this in the Memoranda for 1978.

This joint effort can be viewed as a cooperation within the body of the Global Atmospheric Aerosol-Radiation Experiment (GAAREX), and as such, should be the first step to realization of the proposed program.

The composite studies of atmospheric aerosol enabled one to obtain more extensive information about the tropospheric and stratospheric aerosol. Simultaneous use of dustsondes, impactors and air filters, to study the particle microstructure and chemical composition, promoted the fulfillment of this task. Of great importance were the simultaneous measurements of aerosol parameters and of various qualitative characteristics of the radiation field of the atmosphere using surface and airborne instruments. The comparison of the observed and theoretical vertical profiles of shortwave radiation divergences was a significant part of the program.

The results obtained enabled one to draw the conclusion that the atmospheric aerosol has a complicated nature and its properties are widely at variance. This emphasizes the conventionality of "average" aerosol models and the necessity of further studies of both the aerosol as a whole and its fractions. While the dominating scattering fractions of aerosol (sulfates, SiO_2, etc.) are well known, quite different is the case of the absorbing fractions which are small in mass. In this connection, the differentiated measurements of microstructure and optical properties of different aerosol fractions is of great importance.

The presence of aerosol of different origin in the atmosphere (mineral particles of soil; sulfate particles formed from sulfurous gas; organic and anthropogenic components, etc.) poses the urgent problem of studying aerosol sources and sinks. This complicated problem can be solved only upon the accomplishment of composite observation programs which involve remote sensing at the surface and from space, as well as direct measurements of aerosol and some gaseous components of the atmosphere near the surface and in the free atmosphere.

The observation program should be combined with theoretical modeling of aerosol sources and sinks and the processes of global particle diffusion in the troposphere and stratosphere. The program of the GAAREX is an example of the complex approach to the solution of the problem of atmospheric aerosol and to the evaluation of its impact on climate.

Signed in Leningrad 25 November 1977:

K. Kondratyev
Professor
The Voyeykov Main
Geophysical Observatory

D. J. Hofmann
Professor
University of Wyoming

J. M. Rosen
Professor
University of Wyoming

APPENDIX 1

LIST OF PARTICIPANTS
OF THE MEETING OF THE USA/USSR EXPERTS
ON THE RESULTS OF THE STRATOSPHERIC
AEROSOL STUDIES

20-26 November, 1977, Leningrad
Voeikov Main Geophysical Observatory

Professor J. M. Rosen	University of Wyoming
Professor D. J. Hofmann	University of Wyoming
Professor E. Borisenkov	MGO, Director
Professor V. Stepanenko	MGO, Deputy Director
Professor K. Kondratyev	MGO, Chief of Department, Scientific Supervisor of the experiment on the Soviet side
Dr. N. Ter-Markaryants	MGO, Chief of Laboratory
Professor I. Karol	MGO, Chief of Department, Scientific Supervisor of Project II of WG 8.
Dr. A. Laktionov	Institute of Applied Geophysics, Chief of Laboratory, Scientific Supervisor of the Soviet team
Dr. L. Ivlev	University of Leningrad
Dr. V. Binenko	MGO
Mr. B. Vdovin	MGO
Dr. N. Zaitseva	CAO
Mr. V. Ivanov	MGO
Mr. V. Korzov	MGO
Dr. O. Barteneva	University of Leningrad
Mr. N. Kjome	University of Wyoming
Dr. V. Shlyakhov	MGO

APPENDIX 2

COMPARISON OF RESULTS OBTAINED DURING THE USSR-USA COOPERATIVE AEROSOL MEASUREMENT PROGRAM IN LARAMIE

In the summer of 1975, a cooperative field experiment was conducted in Rylsk, USSR, for the purpose of comparing the vertical profile of aerosol as determined by two different techniques: the impactor method (USSR) and an optical counter method (USA). The experiment was repeated in the summer of 1976, at Laramie, Wyoming. The USSR field party included A. Laktionov, of the Institute of Applied Geophysics (Moscow), and V. Ivanov, V. Binenko, B. Vdovin and V. Korzov, of the Main Geophysical Observatory (Leningrad). The USA group consisted of D. Hofmann, J. Rosen, N. Kjome, G. Olson, and D. Martell of the University of Wyoming. In all, a total of three successful balloon sounding comparisons were made. In this Appendix, we will describe typical results from one of the Laramie soundings.

Composite profiles for comparison of similar data obtained by the two techniques are shown in Figures 1 and 2. In these figures, the impactor results are shown by the heavier curve and the optical counter results are shown by the lighter curve. Figure 1 refers to the concentration of particles with radii $\geq$ 0.2 μm for the impactor and $\geq$ 0.15 μm for the optical counter (the smallest size range observed by the two techniques), while Figure 2 refers to the concentration of particles with radii $\geq$ 0.25 μm in both cases.

It is clear that there is good general agreement between the two methods for smaller particles (Figure 1) in the troposphere. No comparison below 500 mb has been attempted. At an altitude of about 130 mb in Figure 1, there is a significant discrepancy between the two techniques. In this region, the optical counter experienced sporadic high concentrations of aerosol, which was attributed to aerosol expiration of the combined equipment, and therefore, was not included in the analysis of the optical counter but is present in the impactor data. Thus, the dis-

crepancy could be explained in terms of local aerosol pollution from the instrument package.

In the stratosphere, above 15 km, the profiles obtained by the two methods in the case of smaller particles (Figure 1) are quite similar, but the absolute concentration as measured by the impactor is about a factor of 3 smaller than that measured by the optical particle counter. It is tempting to attribute the basis for this disagreement, and for the impactor inconsistency indicated earlier, to the known volatile nature of the stratospheric aerosol. However, this explanation does not seem consistent with the results that will be discussed later. Part of the discrepancy can certainly be accounted for in the different size of particles corresponding to the profile in Figure 1. The optical particle counter can more easily detect the more numerous smaller particles. This is not surprising, since the 0.2 μm radius particles seen in the impactor sample are at the very limit of detection with the optical microscopes employed in analyzing the impactor samples.

The comparison of profiles of larger size particles ($r \geq 0.25$ μm), as shown in Figure 2, is not as good as for the smaller particles. Here the impactor results in the troposphere show a higher concentration of aerosol than the optical particle counter. The difference, however, is not very significant. When working with particles large enough for good resolution under the optical microscope, a conglomerate is sometimes counted as multiple particles in the impactor method and as one particle by the optical counter. Thus, the impactor method could give somewhat larger apparent concentrations. In the stratosphere, where the particles are mostly liquid, this effect would probably be insignificant.

These results have led us to the tentative conclusion that when the particles of interest are large enough to be easily resolved under the optical microscope, the agreement between the two methods is reasonably good. For particle sizes bordering on the resolution of the optical microscope, the absolute agreement between the two methods may not be as good. In Figure 1, for instance, the more opaque particles of the troposphere were apparently seen in the microscope well enough to be counted, while the

fairly transparent stratospheric particles were difficult to see and could not be counted with high accuracy.

To the knowledge of the investigators in this cooperative program, this was the first comparison of particle counting techniques and optical microscope techniques. The latter, in contrast to electron microscope analysis, has some advantages in that if the particles are volatile, their nature will not be altered by analysis. However, the lower size limit for optical microscopes is somewhat of a disadvantage, as is the inability to see liquid particles easily. In general, however, it is a joint feeling that the comparison was a useful undertaking, with results which will be of value in directing future cooperative work. It is also our feeling that the spirit of cooperation necessary in such a program and displayed by the participants throughout the two years of this cooperative effort, should set an example for such future efforts.

FIGURE CAPTIONS

Fig. 1 A comparison of the impactor results ($r \geq 0.20$ μm; thick line) with the photoelectric particle counter results ($r \geq 0.15$ μm and thin line) for 4 Aug., 1976.

Fig. 2 A comparison of the impactor results ($r \geq 0.25$ μm; thick line) with the photoelectric particle counter results ($r \geq 0.25$ μm and thin line) for 4 Aug., 1976.

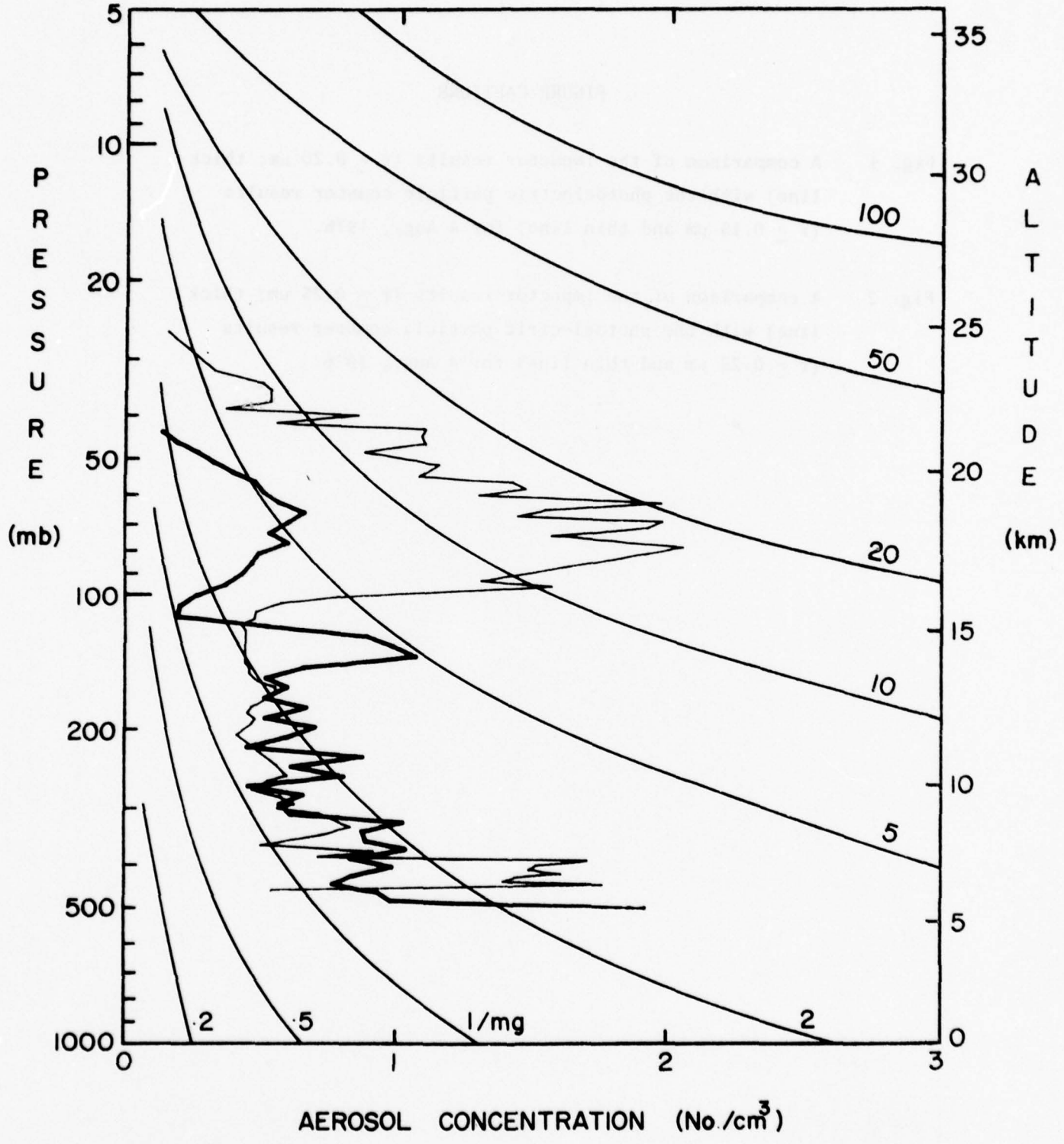
PRESSURE (mb)
ALTITUDE (km)
5
10
20
50
100
200
500
1000
35
30
25
20
15
10
5
0
100
50
20
10
5
2
.2
.5
1/mg
0
1
2
3
AEROSOL CONCENTRATION (No./cm3)

FIGURE 1

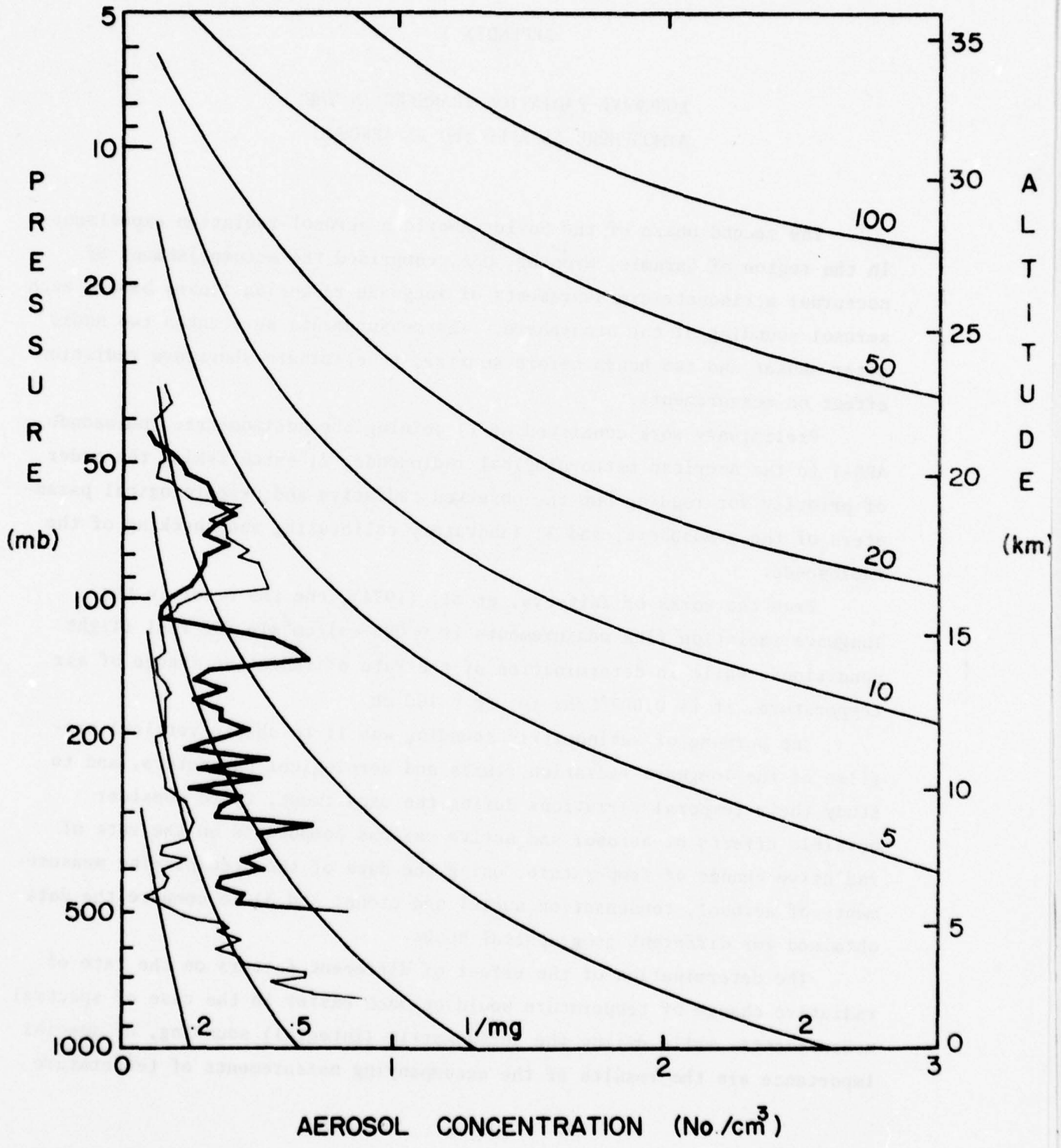
PRESSURE (mb)
ALTITUDE (km)
AEROSOL CONCENTRATION (No./cm³)
5
10
20
50
100
200
500
1000
0
1
2
3
35
30
25
20
15
10
5
0
100
50
20
10
5
2
1/mg
.5
.2

FIGURE 2

APPENDIX 3

LONGWAVE RADIATION TRANSFER IN THE ATMOSPHERE AS AFFECTED BY AEROSOL

The second phase of the Soviet-American aerosol-radiation experiment in the region of Laramie, Wyoming, USA, comprised the accomplishment of nocturnal actinometric measurements of longwave radiation fluxes before each aerosol sounding of the atmosphere. The measurements were taken two hours after sunset and two hours before sunrise, to eliminate shortwave radiation effect on measurements.

Preliminary work consisted of 1) joining the actinometric radiosonde ARS-1 to the American meteorological radiosonde; 2) establishing the order of priority for reading out the observed radiative and meteorological parameters of the atmosphere, and 3) laboratory calibrating and checking of the radiosonde.

From the works of Zaitseva, et al, (1974), the rms error in the longwave radiation flux measurements is 0.005 cal/cm^{2}min for real flight conditions, while in determination of the rate of radiative change of air temperature, it is $0.007°C/hr$ for $\Delta p = 100$ mb.

The purpose of actinometric sounding was 1) to obtain vertical profiles of the longwave radiation fluxes and aerological parameters, and to study their temporal variations during the experiment; 2) to consider possible effects of aerosol and active gaseous components on the rate of radiative change of temperature, using the data of the accompanying measurements of aerosol, condensation nuclei and ozone; and 3) to compare the data obtained for different geographical zones.

The determination of the effect of different factors on the rate of radiative change of temperature would be much easier in the case of spectral measurements, while during the actinometric (integral) sounding, of special importance are the results of the accompanying measurements of temperature

stratification, in particular, and the data on the content of water vapor, aerosol, ozone and other active gaseous components of the atmosphere, such as CO_2, etc.

These data and the results of numerical modeling, as applied to experimental conditions, enable one to quantitatively evaluate the effect of aerosol and other factors on the longwave radiation transfer in the atmosphere. Table 1 of the USSR Report (Appendix 5) lists the information about the launches of actinometric radiosondes. The launches were carried out in clear skies (clouds not exceeding 2-3 p.) and low wind. The geographical coordinates for the balloon measurement area were 41°2'N, 105°W, and the altitude was 2000 m above sea level.

The cyclonic activity during the aerosol-radiation experiment lowered the altitude of the tropopause. On August 31, 1976, it was at the level of 120-130 mb; then the tropopause became stratified and lowered down to 160-180 mb (Tables 2 through 6 of Appendix 5). This fact is of special interest, since the altitude of the tropopause significantly affects the vertical profile of aerosol concentration in the lower atmosphere and upper troposphere.

The aerosol layers in this part of the atmosphere are partially due to exchange processes at the tropopause and volcanic activity (Pinnick, et al, 1976). Here, a change in the aerosol and ozone profiles and a reduction of the air temperature lapse rate are observed. All this affects the longwave radiation transfer in the atmosphere and the vertical stratification of the aerosol number density (Kondratyev K. Ya., 1956; 1976).

As seen from Figure 1 (a,b,c) and Tables 2 through 6 of Appendix 5, the increase of the effective thermal emission, F, with height is mainly observed and, consequently, radiative cooling takes place. According to the data of the American aerosol sonde, the aerosol layers and radiative heating were observed in the region of inversion and sub-inversion layers and in the tropopause. For example, Figure 1 (a,c) shows the aerosol layer at the level of 460-520 mb, the concentration of particles, the size of which exceeds 0.3 μm, being 3 cm^{-3}. Here, at the base of the temperature inversion, radiative heating up to 0.43°C/hr is observed with the following strong radiative cooling down to 1.13°C/hr.

In the lower stratosphere, at the level of 70-80 mb, the aerosol particle concentration reached 1.8 cm^{-3}, but a sharp increase of the thermodynamic temperature in this region and the additional effect of ozone absorption have led to radiative heating up to 0.27°C/hr in the lower part of the aerosol layer and to radiative cooling down to 0.06°C/hr in its upper part.

The same vertical profile of the rate of radiative change of temperature and aerosol number density can be seen in Figure 1 (b,c). The aerosol and radiation measurements showed that the highest content of dust in the atmosphere was observed on July 31, and August 4, 1976 (as compared to August 6, 1976), and on August 5, 1976 (one of the launches after sunset).

The difference in the vertical profiles of radiation parameters before dawn and after sunset is apparently associated with transformation of meteorological conditions. But it is difficult to interpret with only five launches as a basis (Figure 2 (a,b)).

We may draw a conclusion from the available data that the aerosol layer can be compared to the radiative model of a cloud which has active radiative boundary layers. In the middle of the layer, the radiative change of temperature is close to zero, i.e., thermodynamic equilibrium takes place, while the upper boundary corresponds to a heat sink and the lower boundary to a heat source.

Comparison of the vertical profiles of aerosol obtained from the photoelectric measurement data and radiative properties of the atmosphere for the corresponding periods, shows that the aerosol layers change the sign of the rate of radiative change of temperature. The latter fact may be an indirect indication of aerosol in actinometric samples.

An attempt has been made on the basis of available data to plot the rate of radiative change of temperature versus aerosol concentration (with particle's diameter exceeding 0.3 μm) at the corresponding altitudes in the layer above 300 mb (in order to eliminate the effect of water vapor, the main fraction of which is in the troposphere). It is seen from Figure 3 that correlation between these parameters is rather weak, which can be explained by 1) difficulties in determination of the altitudes of actinometric

and aerosol sondes launched at different times; 2) different nature of the aerosol optical activity in different regions of the longwave radiation spectrum; and 3) the effect of meteorological factors, such as variability of the vertical profile of humidity and gaseous components in the atmosphere.

Probably, this correlation is more stable in the atmospheric window. Comparison of the results of actinometric sounding carried out in Rylsk and Laramie has shown their similarity, but in the case of Laramie measurements, the above mentioned peculiarities in the longwave radiation transfer manifest themselves most clearly. In the layer of temperature inversion, in the region of the tropopause, the aerosol layer approximates a cloud as to its absorbing and emitting properties, but in some cases of optically active aerosol it may be equivalent to a blackbody.

The thin layers with alternating heating and cooling have already been detected in the cloud-free atmosphere from the data of previous actinometric soundings.

The results of this experiment enable one to suppose that the radiative properties of the atmosphere are determined by thin layers with increased concentration of optically active aerosol.

Thus, the results obtained from the Soviet-American experiment make it possible to speak about good qualitative fitting of the data on aerosol concentration in the atmosphere and atmospheric radiative properties. It is rather advisable that a joint detailed analysis of these data be performed in order to quantitatively evaluate the discovered effects.

REFERENCES

Kondratyev, K.Ya., "Climate and Aerosol," Trudy GGO, issue 381, p. 3-66, 1976.

Kondratyev, K. Ya., "Radiative Heat Exchange in Atmosphere," Gidrometeoizdat, p. 423, 1956.

Pinnick, R.G., J. M. Rosen and D. J. Hofmann, "Stratospheric Aerosol Measurements," J. Atmos. Sci., 32, p.1457-1462, 1976.

Zaitseva, N. A. and G. N. Kostyanoy, "Longwave Radiation Field in the Free Atmosphere," Gidrometeoizdat, p. 148, 1974.

FIGURE CAPTIONS

Fig. 1 Vertical profiles of radiative change of temperature (——), aerosol concentration (...), and aerosol mixing ratio (---). a - W-126,127; b - W-129,130; c - W-132,133.

Fig. 2. Vertical profiles of temperature, (... - W-128,131; -.-.- W-129,132), and the rate of radiative change of temperature, (—— W-128,131; --- W-129,132). a - W-128,129; b - W-131,132.

Fig. 3. Rate of radiative heating of the atmosphere vs. aerosol number density.

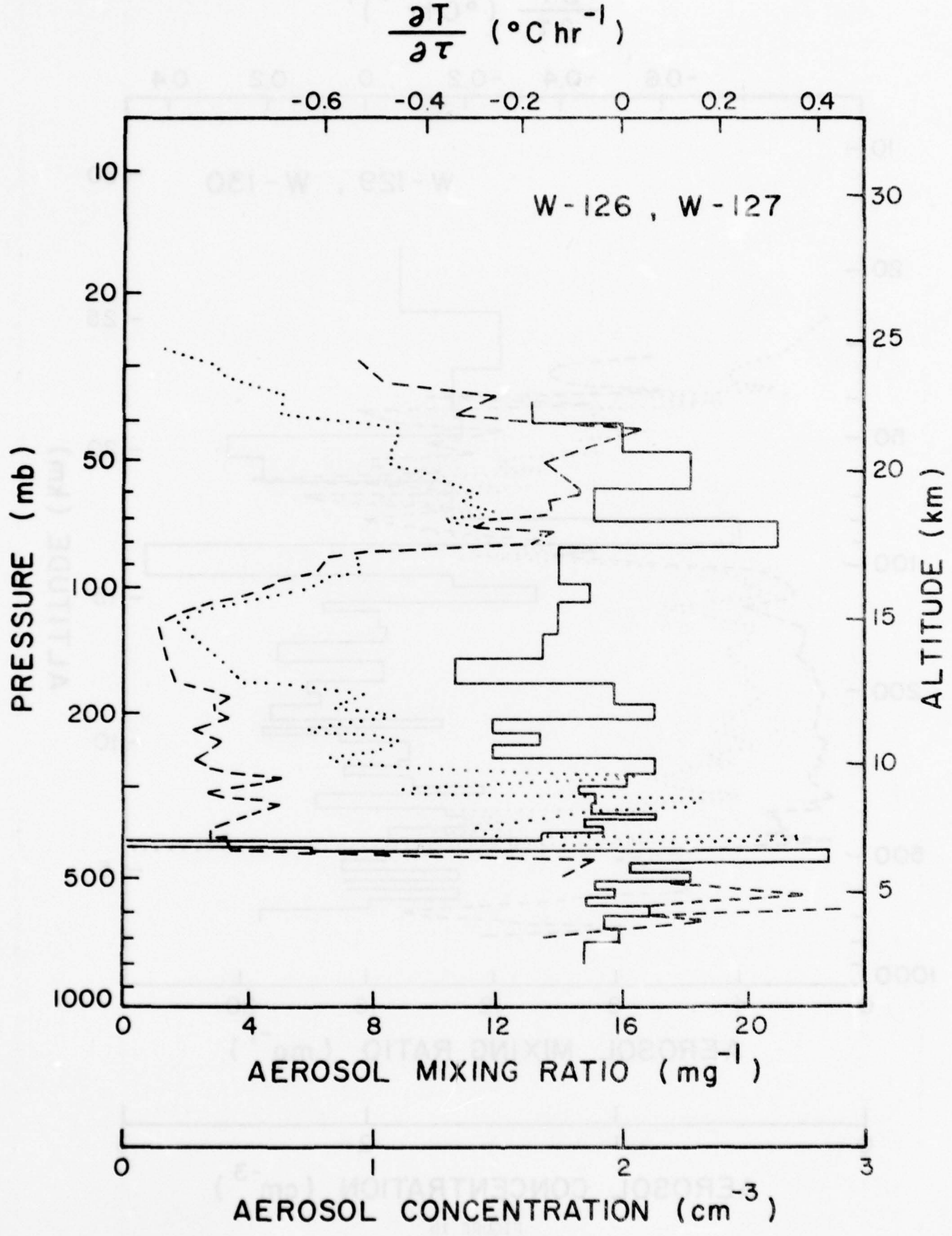
$\frac{\partial T}{\partial \tau}$ (°C hr^{-1})
-0.6
-0.4
-0.2
0
0.2
0.4
W-126 , W-127
PRESSURE (mb)
10
20
50
100
200
500
1000
ALTITUDE (km)
30
25
20
15
10
5
0
4
8
12
16
20
AEROSOL MIXING RATIO (mg^{-1})
0
1
2
3
AEROSOL CONCENTRATION (cm^{-3})

FIGURE 1a

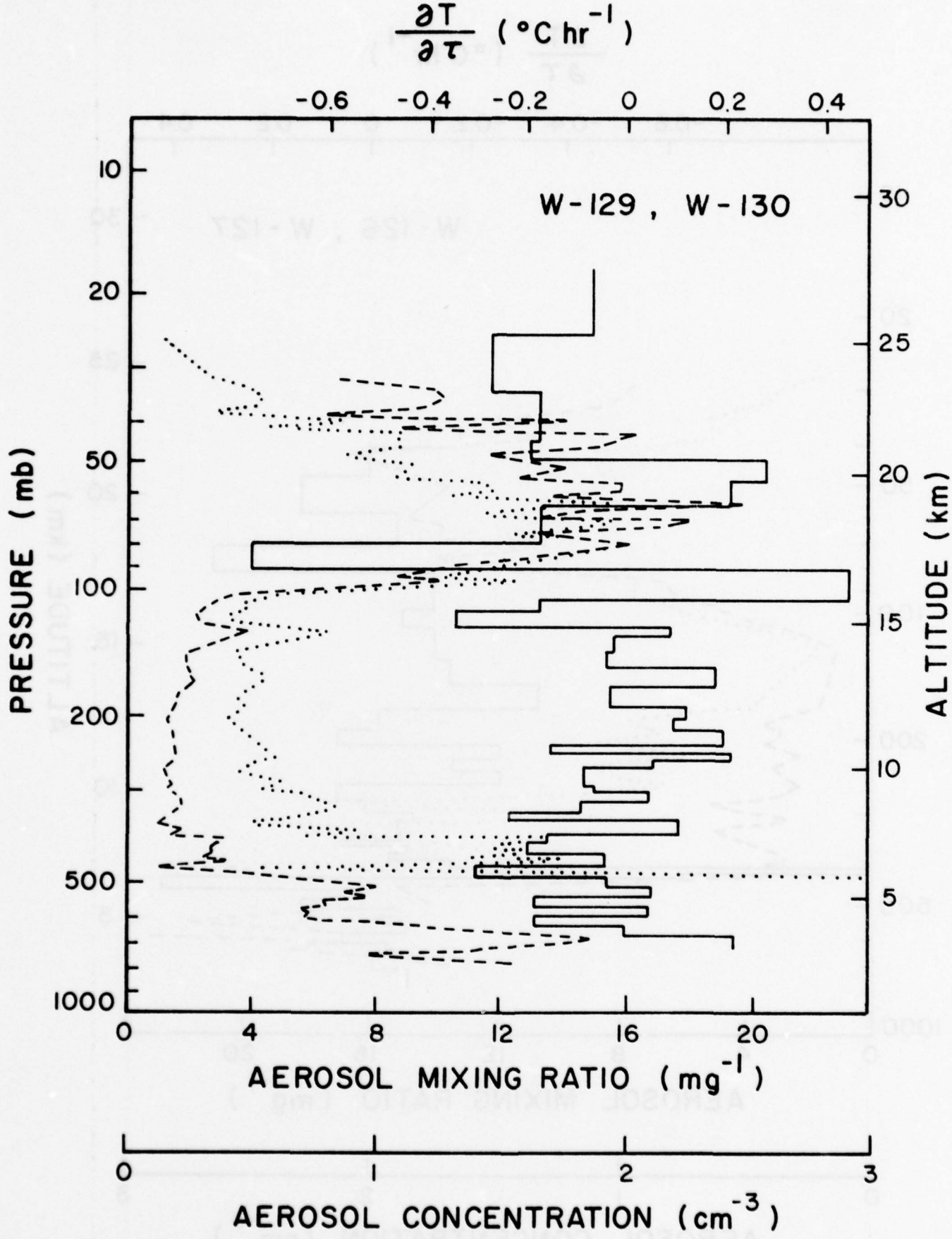
$\frac{\partial T}{\partial \tau}$ (°C hr^{-1})
-0.6
-0.4
-0.2
0
0.2
0.4
W-129, W-130
PRESSURE (mb)
10
20
50
100
200
500
1000
ALTITUDE (km)
30
25
20
15
10
5
0
4
8
12
16
20
AEROSOL MIXING RATIO (mg^{-1})
0
1
2
3
AEROSOL CONCENTRATION (cm^{-3})

FIGURE 1b

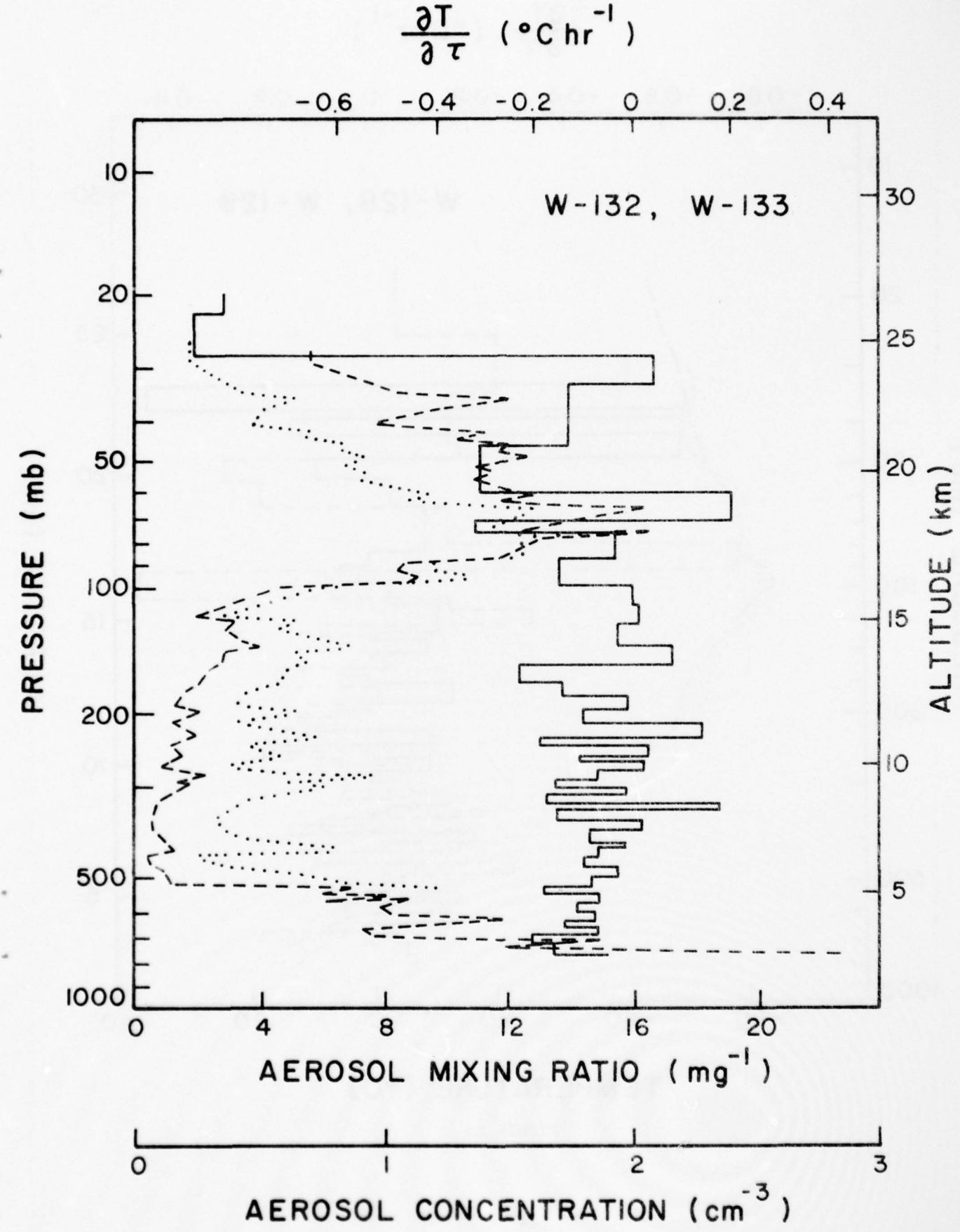
$\frac{\partial T}{\partial \tau}$ (°C hr^{-1})
-0.6
-0.4
-0.2
0
0.2
0.4
W-132, W-133
10
20
50
100
200
500
1000
30
25
20
15
10
5
PRESSURE (mb)
ALTITUDE (km)
0
4
8
12
16
20
AEROSOL MIXING RATIO (mg^{-1})
0
1
2
3
AEROSOL CONCENTRATION (cm^{-3})

FIGURE 1c

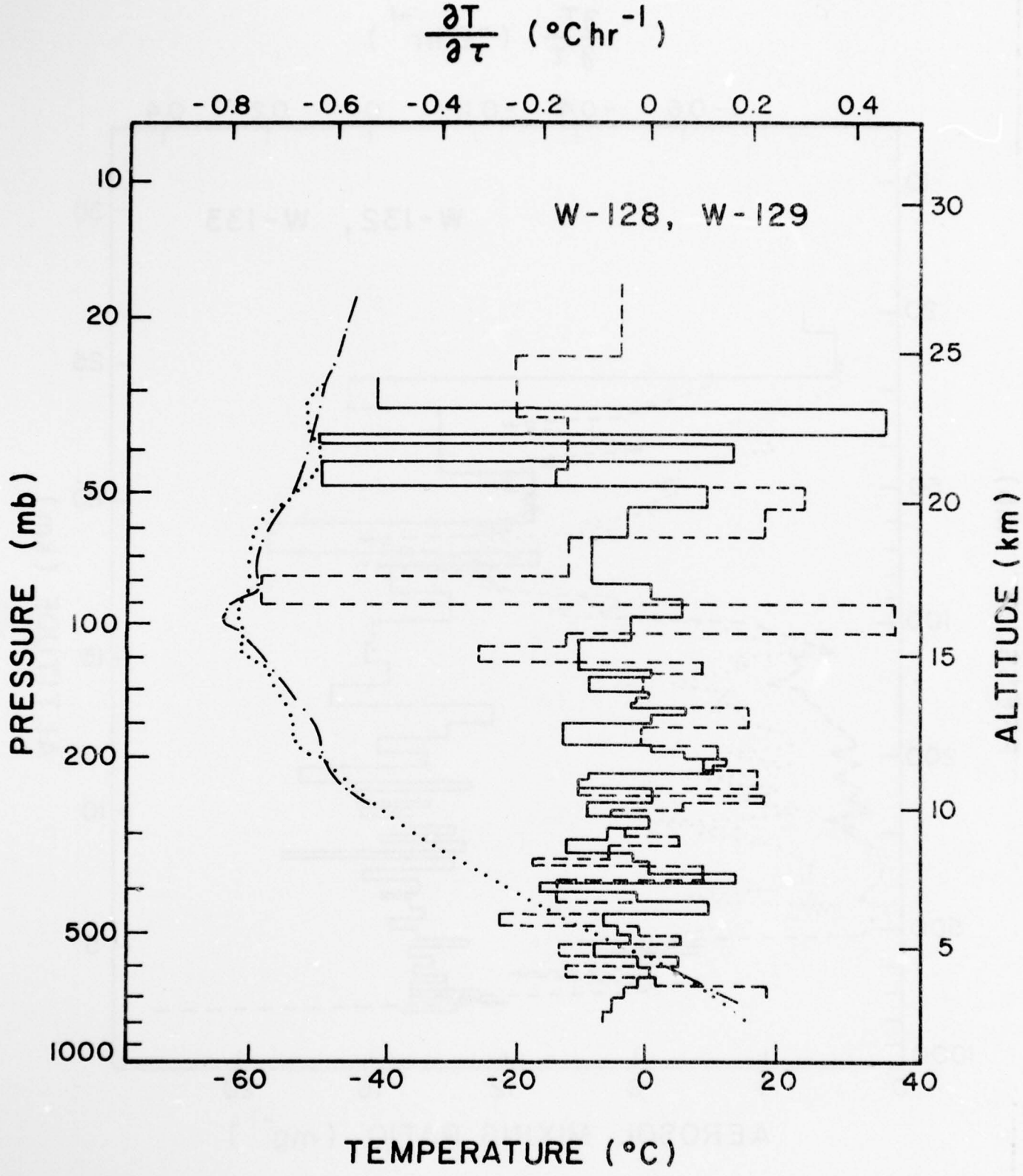
$\frac{\partial T}{\partial \tau}$ (°C hr^{-1})
-0.8
-0.6
-0.4
-0.2
0
0.2
0.4
W-128, W-129
10
20
50
100
200
500
1000
PRESSURE (mb)
30
25
20
15
10
5
ALTITUDE (km)
-60
-40
-20
0
20
40
TEMPERATURE (°C)

FIGURE 2a

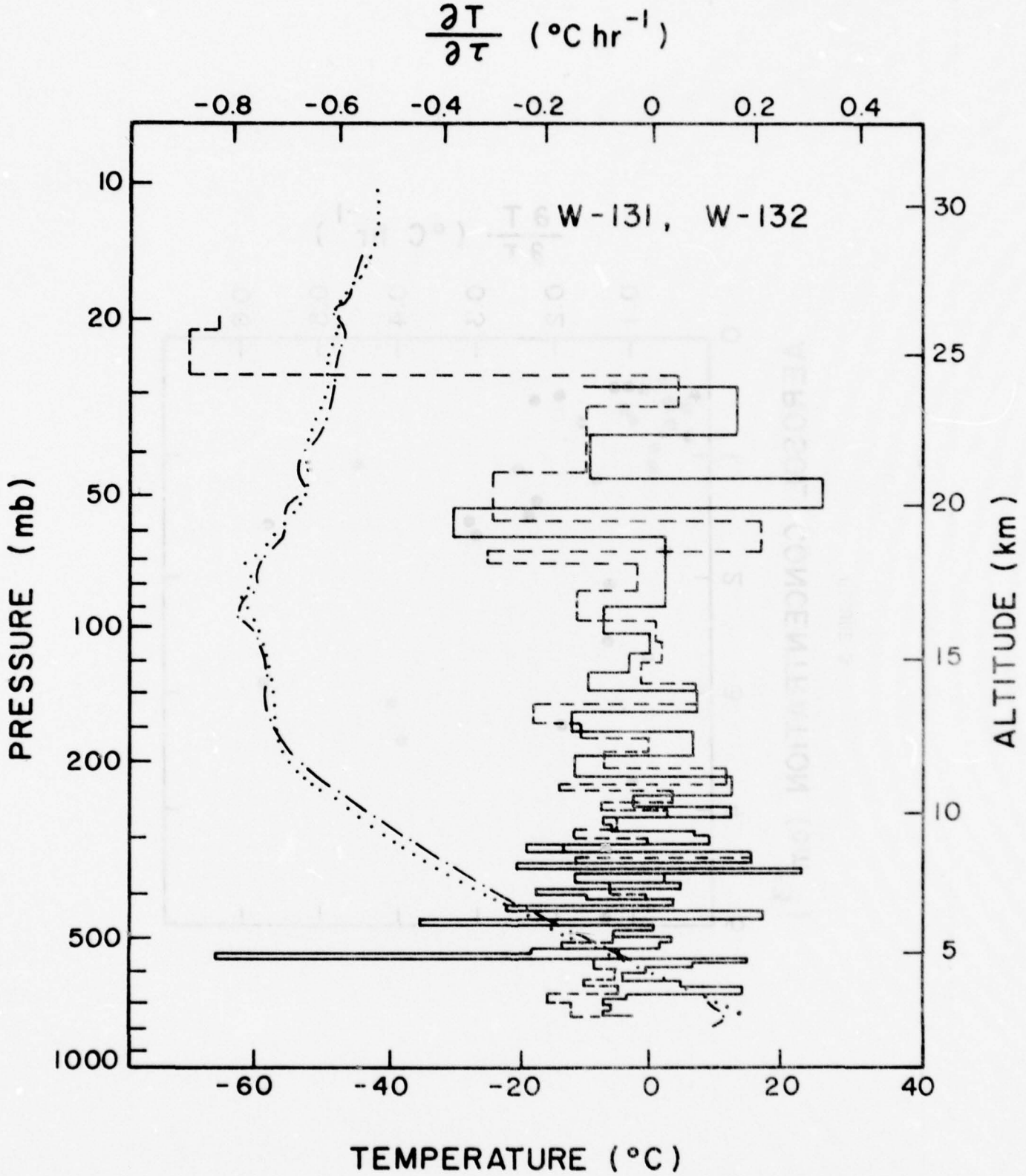
$\frac{\partial T}{\partial \tau}$ (°C hr^{-1})
-0.8
-0.6
-0.4
-0.2
0
0.2
0.4
W-131, W-132
PRESSURE (mb)
10
20
50
100
200
500
1000
ALTITUDE (km)
30
25
20
15
10
5
-60
-40
-20
0
20
40
TEMPERATURE (°C)

FIGURE 2b

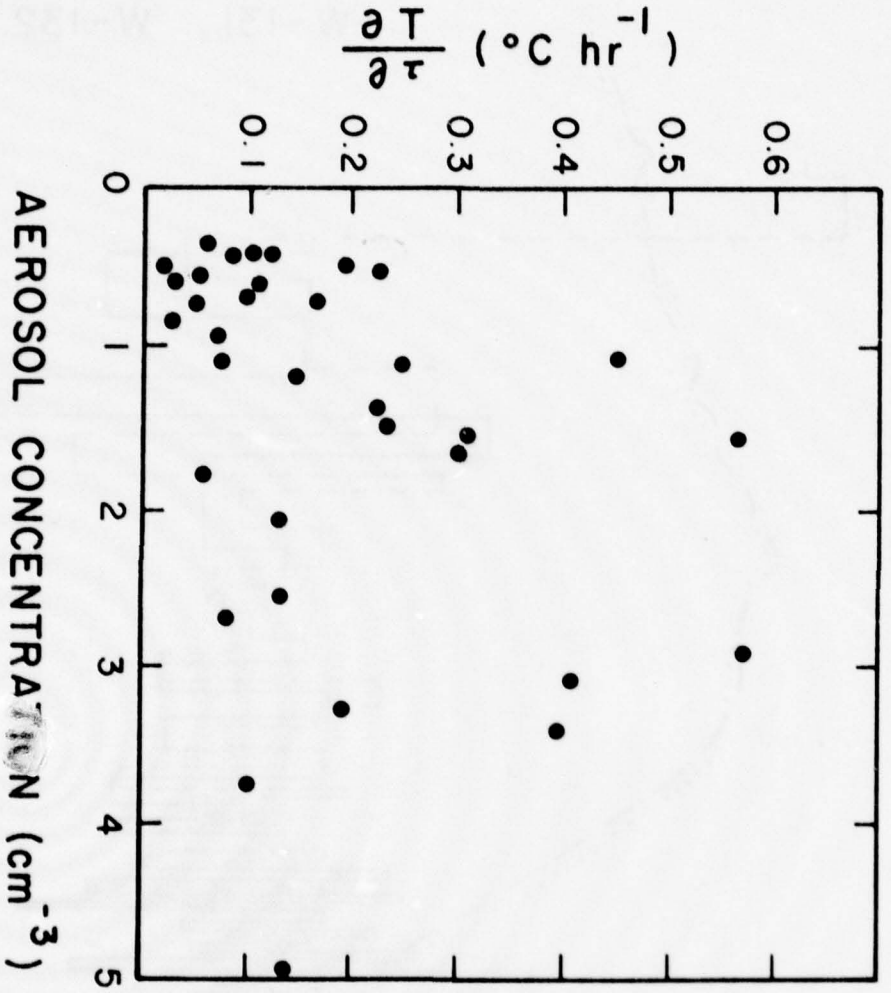
$\frac{\partial T}{\partial t}$ (°C hr^{-1})
0.1
0.2
0.3
0.4
0.5
0.6
0
1
2
3
4
5
AEROSOL CONCENTRATION (cm^{-3})

FIGURE 3

APPENDIX 4

SOVIET-AMERICAN AEROSOL-RADIATION EXPERIMENT IN RYLSK

FORWARD

In spite of a vast amount of experimental data available on the vertical structure of atmospheric aerosol (Kondratyev, 1974; Ivlev, 1972; Zuev, 1973 and Rosen, 1969), as well as data concerning radiation parameters of the whole atmosphere and individual layers (Vasilyev, 1973 and Zaitseva, 1971), there is no close correlation between data on aerosol structure obtained by different techniques and radiation parameters of the atmosphere. Optical aerosol models, in particular, generally lack an adequate experimental background on aerosol microstructure. Therefore, a set of aerosol and radiation measurements is particularly desirable. These measurements involve data collection on aerosol structure and atmospheric radiation parameters for a specific location and season, and they are, in themselves, useful and relevant.

A wide range of optical measurements and those of aerosol microstructure using ground, airborne and balloon-borne equipment was conducted in Rylsk, USSR, in August of 1975, which provided data to solve the above problem.

WEATHER CONDITIONS DURING THE EXPERIMENT

Rylsk is situated in an area of weak cyclonic activity. Atlantic cyclones over Europe are subject to significant changes and occlusion. As a result of these phenomena, a low gradient pressure field is generally observed in these areas during the months of July and August.

The synoptic situation was characterized by cold air flows from the polar regions of Barents and White Seas and warm tropical air flows from Asia Minor. An old cyclone, originated at the interface of the above

flows, reached the Rylsk area by August 1. A cyclonic vortex was traced throughout the troposphere. On August 4 and 5, a change in the natural synoptic period occurred. On August 5, weather conditions were modified by an intermediate pressure ridge and a re-establishment of upper northeast winds. An intensification of downward vertical fluxes occurred. Changeable weather and extended cumulus cloudiness was due to further development of the synoptic situation. Some difficulties concerning ground measurements and radiation data interpretation, as well as measurements in the free atmosphere, were caused by unfavorable weather conditions.

GROUND MEASUREMENTS

A set of ground aerosol meteorological and radiation measurements gives a general outline of the atmospheric situation during the experiment and enables one to compare capabilities of various approaches to the studies of optical and aerosol characteristics of the atmosphere.

Instrumentation

Ground studies involved routine measurements of radiation balance and its components; direct, scattered and global radiation. These measurements were carried out with two albedometers, balance meters designed by Yanishevsky (1969), and integral and ground longwave net radiometers designed by Shlyakhov (1969). In addition, spectral measurements of downward radiation in the atmospheric "window" of 8-12 μm were taken.

A set of measurements of optical characteristics was conducted. They included integral and spectral transparency of the atmosphere; water vapor content in the atmospheric column, atmospheric horizontal transparency (meteorological visibility range), and degree of polarization. Measurements of solar radiation scattering at small angles were also made.

The atmospheric integral transparency, reduced to m=2, was calculated from direct radiation data obtained with an AT-50 actinometer.

To measure the spectral aerosol optical thickness of the atmosphere over the spectral range of 0.35-1 μm, a modified Feisner actinometer was used with eleven interference filters cutting off narrow spectral bands

($\Delta\lambda$ = 0.07 - 0.10 μm), and was practically free of selective absorption of radiation by gasses and water vapor. The filter with λ_{max} = 0.942, adjusted to the water-vapor absorption band $\rho\sigma\tau$, enabled one to use the device as an optical hygrometer (Kondratyev, 1973). The horizontal atmospheric transparency, or the meteorological visibility S (S = $3/\alpha$ where α is the coefficient of light scattering per km), was recorded with a photoelectric nephelometer (Polevitsky, 1972).

To measure the degree of day sky polarization at the point of maximum polarization, a visual polarimeter (λ_{eff} = 0.533) and a photoelectric polarimeter with five interference filters were used in the visible and near infrared spectrum region from λ = 0.3 μm to λ = 1 μm.

Measurements of the spectrum of particle size and chemical composition of atmospheric aerosol in the surface atmospheric layer were taken at different levels and different points about 1.5 km apart (Ivlev, 1970; Prokofyev, 1972).

In conjunction with aerosol sampling, lidar measurements of backward scattering and depolarization coefficients were performed. The observations were carried out on the days of aerosol sonde launches, according to the following program. The actinometric observations and observations of meteorological visibility were made at 30-minute intervals; the aerosol sampling was carried out at 1-hour intervals. Whenever possible, measurements of radiation characteristics of the whole atmospheric thickness were taken.

Discussion of the Results and Data Analysis

The day-time course of optical and meteorological characteristics of the atmosphere on August 1, 3 and 5 is shown in Figure 1. No anomalies can be found in correlations between various optical parameters (optical thickness, horizontal atmospheric transparency, aerosol extinction) and meteorological characteristics. Representative spectral variations of aerosol optical thickness on August 1, 3, 5 and 6 are reproduced in Figure 2. These curves are fitted by the equation $\tau^*_\lambda = \beta\lambda^{-n}$, which describes solar

radiation extinction due to aerosol in a moist atmosphere. The exponent n varied between 0.9 and 0.3, which corresponds to a water content of 1.8 - 3.5 cm.

Significant turbidity, observed during the experiment, should be noted. The mean value of the integral transparency P was about 0.65; sometimes the aerosol optical thickness was as high as 0.60 at λ = 0.35 μm and 0.23 at λ = 1 μm. The degree of day sky polarization at the point of maximum polarization did not exceed 0.45 under cloudless conditions.

Low atmospheric transparency is a regular characteristic of the area (Pivovarova, 1969). This feature is connected with both industrial air pollution and fog formation and dispersion in the floodlands of the Seim River situated nearby.

An analysis of $\tau^*(\lambda)$ has shown that in the shortwave spectrum region, a deviation from λ^{-n} was observed twice during this period (with northwest surface winds and at $P_2 \geq 0.72$). The overestimated values of $\tau^*(\lambda)$ might be caused by radiation absorption by ferric oxide particles, the presence of which is natural in this industrial area. At $P_2 > 0.70$, there was no deviation from the above law which agreed favorably with the data cited by Barteneva (1976).

An aerosol absorption effect can be confirmed from the deformed curves of the diurnal variations of P_{max} observed during individual cloudless periods, the value of $\tau^*(\lambda)$ being constant. However, due to a lack of long-term observations and meteorological conditions unfavorable for determination of the atmospheric optical characteristics, one cannot reliably estimate an aerosol absorption.

Surface lidar aerosol measurements were made in the horizontal direction only at the ruby emission wavelength (639 ηm). Included in lidar measurements were diurnal variations of the depolarization coefficient d(t) in the atmospheric surface layer and spatial distribution of this quantitiy, d(R), along specified paths. The diurnal variations of d reflect changes in aerosol particle microstructure; namely, transformation from a non-spherical shape to a spherical one.

The maximum value of d (0.2-0.3), observed around noon, corresponds to the most dusty atmosphere, while a minimum value observed at night and early

morning, corresponds to a decrease in dust particles in the surface layer and to their partial water coating and subsequent transition to spherical shape.

Aerosol was sampled at three different points - the balloon launching site, the solar radiation observing site and the meteorological observing site. The difference in elevation of the first and third sites was about 40 m. At the latter site, sampling was made at 1, 2, 5 and 8 m above ground level. Measurements of aerosol microphysical parameters in the surface layer were taken using polyvinylchloride filters, which make it possible to carry out chemical analysis and gain information on microstructure with optical and electron microscopes.

Chemical composition, number density, size distribution and morphological structure of aerosol particles were analyzed over a twenty four hour period at different levels. These data made it possible to evaluate the input of local surface sources into the vertical structure of atmospheric aerosol, as well as to calculate the optical characteristics of the surface aerosol. Typical data on the particle's chemical composition, size distribution and number density in the surface layer over the Rylsk area for the summer period are given in Table 1. Analysis of the data leads to the following conclusions:

1. The main part of the surface layer aerosol is of soil origin.
2. Powerful convective transfer of aerosol into the troposphere is characteristic for the given observational conditions.
3. A diurnal variation of the aerosol content in the surface layer is observed, which is associated with particle generation in the morning and day hours with subsequent development of turbulence and convection.

   Two maxima in particle concentration are distinctly observed in morning to noon and in the evening hours. A particularly high concentration of soil dust was observed over the meteorological site ($\rho \simeq 0.5$ mg m^{-3}), which is to a great extent associated with wind erosion of top soils.

   The strange variability of aerosol content in the lower troposphere and in the surface layer is obviously connected, not only

with diurnal variations of particle generation processes, but with washing out of particles by clouds and by precipitation as well.

4. Comparison of the microphysical data with measurements in previous years shows that although no significant changes in the surface aerosol structure occurred, a small change in the particle size distribution was observed. The secondary maximum of the particle size distribution, which fell in the 2-4 μm range during the 1967 - 1969 measurements, shifted to 3 to 5 μm for the present experiment. This observation agrees with data obtained from corona photometer measurements of solar radiation scattered at small angles.

   The electron microscope analysis provided a detailed study of the particle's morphological structure and the influence of ambient air parameters on it. In particular, the particles with a liquid coating, which left circular traces after evaporating, were found to be present in samples taken at relative humidities far from saturation (~ 80%). In addition, a transition of the size distribution maximum, from the size range 0.01 - 0.05 μm to 0.05 - 0.1 μm, was observed when relative humidity increased from 80% to 95%.

   In the range of particle radii larger than 0.5 μm, almost all of the particles were of irregular shape and were mainly of soil origin.

The strange variability of aerosol content in the lower troposphere and in the surface layer is obviously connected, not only with diurnal variations of particle generation processes, but with washing out of particles by clouds and by precipitation as well.

4. Comparison of the microphysical data with measurements in previous years shows that although no significant changes in the surface aerosol structure occurred, a small change in the particle size distribution was observed. The secondary maximum of the particle size distribution, which fell in the 2 - 4 μm range during the 1967-69 measurements, shifted to 3 to 5 μm for the present experiment. This observation agrees with data obtained from corona photometer measurements of solar radiation scattered at small angles.

   The electron microscope analysis provided a detailed study of the particle's morphological structure and the influence of ambient air parameters on it. In particular, the particles with a liquid coating, which left circular traces after evaporating, were found to be present in samples taken at relative humidities far from saturation (~80%). In addition, a transition of the size distribution maximum, from the size range 0.01 - 0.05 μm to 0.05 - 0.1 μm, was observed when relative humidity increased from 80% to 95%.

   In the range of particle radii larger than 0.5 μm, almost all of the particles were of irregular shape and were mainly of soil origin.

AIRCRAFT MEASUREMENTS

Instrumentation

The instrumentation on board the IL-18 MGO flying laboratory included:

1. A set of instrumentation for obtaining meteorological data.
2. Spectral instrumentation. The spectral measurements were performed with the help of two identical K-2 spectrometers, receiving radiation coming from the lower and upper hemispheres in the wavelength range of 350 - 950 nm (Zaitseva, 1971).
3. Aircraft actinometric complex (Vinogradova, 1973; Dmokhovski, 1972).
4. Aerosol complex A.2 consisting of an impactor and a filter sampler (Dmokhovsky, 1973; Sivkov, 1968).

Discussion of the Results Obtained

Measurements between altitudes of 0.5 km and 7.2 km permitted determination of the absorptivity of this atmospheric layer. The spectral value of aerosol absorption in this layer cannot be singularly determined as it is characteristic of the ferric oxide absorption and varies comparatively little with wavelength. The aerosol absorption of shortwave radiation in this area is obviously determined by the presence of soot particles besides the ferric oxides.

Actinometric measurements have shown that the integral value of aerosol absorption by the 0.5 - 7.2 km layer, in the absence of clouds, was about 2.5%. Spectral measurements in the region of 350 - 450 μm yielded aerosol absorption values reaching 5 to 6%.

Aerosol measurements have shown appreciable spatial inhomogeneity of particle concentration, both in vertical and horizontal directions. In particular, inhomogeneous horizontal structure of aerosol was observed up to 3 - 3.5 km, which was due to the influence of the Seim River upon convective air flows and relative humidity in the lower troposphere. Some results of aircraft measurements of tropospheric aerosol number density, size distribution and chemical composition are given in Tables 2 and 3. It should be noted that the impactor and filter data on size distribution differ significantly, which can be explained by both the aerosol particle nature and differences in sampling techniques.

Fine organic particles are dissolved during the dissolving of the filter fiber in xylene. Droplets of acid solutions, in particular those of sulfuric acid, cannot be seen through the optical microscope, while traces of such droplets are practically always found during electronic microscope survey. The spreading of liquid particles over the substrate is an important factor, also. This can lead to overestimating the particle size, especially for the range of $r > 0.5$ μm.

The tropospheric aerosol chemical composition in the area of Rylsk has no special features. An increased amount of Fe and Al in aerosol matter is observed. Ca is scarce, obviously due to the local soils' composition. Concentrations are significantly lower compared to samples taken over the Kara-Kum desert and the Atlantic to the southwest of the Sahara. The dimen-

sions of particles, which can be identified as Fe 0 , vary widely from r_{min} = 20 - 30 μm, to r_{max} = 250 - 300 μm, in contrast to Kara-Kum samples where the Fe_2O_3 particles were of almost uniform size.

It should be noted that layers of higher concentration of Fe aerosol were observed at certain altitudes. These particles looked brown under the optical microscope and their chemical analysis showed increased content of Fe.

Sulfate concentrations were rather low. The SO_4^{--} content never exceeded 0.2 μg m^{-3} for the 3 to 5 km altitudes.

Electron microscopy of samples shows that the sulfate particles were never larger than r = 0.5 μm. Some particles evaporated under the electron beam. These were of μm size and/or irregular shape. It is most probable that they were of organic origin.

BALLOON MEASUREMENTS

Instrumentation

1. Standard radiosonde capable of providing data on temperature, humidity and wind speed.
2. Night actinometer radiosonde ARZ-1 of the Central Aerological Observatory design. Radiation measurements were performed during night time prior to the morning balloon launches (Ivlev, 1970).
3. Photoelectric particle counter determining the particle concentration in two ranges of $d_1 \geq 0.3$ μm, and $d_2 \geq 0.5$ μm of the University of Wyoming design.
4. Impactor and single use filter device operating continuously above a pre-set altitude (Kondratyev, 1974; Ivlev, 1972; Zuev, 1973).

In the impactor, the particles are deposited on a glass substrate covered with silicon oil. Analysis of impactor samples was performed by means of an optical microscope. It made it possible to obtain the non-volatile particle concentration and size distribution for $r \geq 0.22$ μm.

Polyvinylchloride filter tissue, contributed by the aerosol laboratory of the Karpov Physico-Chemical Institute, was used for the experiment. The analysis of filter samples was made by means of both optical and electron microscopes. The electron microscope made it possible to obtain the aerosol

particle size distribution for the whole stratospheric layer, beginning with a particle size of 0.22 μm, as well as to analyze the samples morphologically. The analysis has shown that the substrate were significantly contaminated with dust from balloons. Balloon particles were comparatively easy to identify under the electron microscope because of their specific microstructure.

Discussion of the Results Obtained

The principal results of aerosol measurements are given in Table 4 and Figure 3. One can point out that there is not complete agreement between the data of all three instruments. It should be noted that the impactor data correlate very well with data on wind speed in the troposphere: maxima of particle concentration correspond to wind speed maxima. The largest discrepancy is in the stratosphere where the impactor indicates smaller concentrations than the dustsonde. As long as the impactor efficiency does not vary much with height, the explanation for this fact should be searched for in the nature of the stratospheric aerosol itself. The electron microscopy of samples shows the presence of spherical particles which evaporate in the electronic microscope and leave "clear spot" traces (Figure 4). If one takes into account the concentration of clear spots and their size distribution for the impactor samples, then the agreement between the photoelectric counter and the impactor data would greatly improve. A particularly good agreement can be reached if one supposes that the dimensions of the "clean spots" are slightly less than the dimensions of the evaporated spheres. It is highly probable that these spheres were, in reality, sulfuric acid droplets, known to exist in the stratosphere. In the case of sulfate particles, some non-evaporated ones would have been observed. Spherical traces, larger than 0.2 μm, were also observed, but in these cases non-volatile intrusions were always present. The question of the possibility of acid droplets smaller than 0.2 μm needs special research, because the physical mechanism blocking their evaporation, is not clear.

The observation of an aerosol layer at 10 km altitude (see Figure 3) is of special interest. The layer may have been due to volcanic eruptions. Calculations of trajectories for dust particles injected to the 200 mb level

during the eruption of Tolbachik volcano (Kamchatka peninsula) shows that these particles could reach the Rylsk area in approximately 10 days. Figure 5 shows a trajectory of dust particles injected to the 200 mb level on July 27, 1975, reaching the Rylsk area on August 5, 1975. Intensive dust outbreaks into the atmosphere by the Tolbachik volcano began approximately July 17-20, 1975, so that volcanic dust could have already reached the Rylsk area by July 31 or August 1.

Intercomparison of data on aerosol particle vertical concentration and longwave up and downwelling radiation flux is interesting (Figure 6). In all three cases of actinometric radiosonde ARZ-1 launches, an air temperature inversion near the surface was observed to diminish the radiative flux variations by 0.015 - 0.05 cal $cm^{-2}min^{-1}$. Radiative heating up to 0.7°C hr^{-1} under the inversion layer was observed during the second launch. Radiative heating was also observed in the higher atmospheric layers. Radiative warming and cooling layers were in turn observed near the tropopause. The $dT/d\tau$ profile indicates the presence of thin air layers within which cooling and heating occur, probably determined by the optical properties of thin aerosol layers. Above 20 km, this effect is obviously influenced by the presence of ozone in the atmosphere and no meaningful correlation between aerosol layers and radiative warming and cooling could be found.

CONCLUSION

The aerosol-radiation experiment, held in Rylsk in the summer of 1975, represents an attempt at a complex approach to determination of aerosol structure, in particular, the stratospheric aerosol. The data on aerosol were obtained by means of simultaneous microphysical and optical measurements; an attempt was made to evaluate the role of aerosol in radiative properties of the atmosphere. The data testify to inadequacy of different techniques for measuring the atmospheric aerosol (e.g., impactor and photoelectric counter), at the same time showing how the information on aerosol is combined if different measurement techniques are simultaneously employed. It is interesting to note that the most satisfactory agreement between the optical and microphysical data on aerosol content in the atmosphere is ob-

served for larger particles ($r > 0.1$ μm) which proves that such particles, present in the cloud-free atmosphere, are mainly non-volatile.

The confirmation of an aerosol layer consisting mainly of liquid particles in the lower stratosphere is a particularly important result. These are probably particles of sulfuric acid. This conclusion is important for understanding the complete physics of the lower stratosphere.

It follows from the available data that aerosol influence on the radiative regime in the upper atmosphere is not a decisive factor.

Experience gained in conducting field research during this joint Soviet and American program will certainly be of great help in future cooperative efforts such as the proposed Global Atmospheric Aerosol Radiation Experiment (GAAREX).

REFERENCES

Barteneva, O. D., L. K. Veselova, N. I. Nikitinskaya, "Influence of Selective Aerosol Absorption on the Optical Characteristic of Atmospheric Thickness at Small Values of Water Vapor Content," in Radiation in the Atmosphere, ed., K. Ya. Kondratyev. Leningrad University Press, p. 58-72, 1976.

Barteneva, O. D., L. K. Veselova, N. I. Nikitinskaya, "Optical Properties of Atmospheric Aerosol over Tropical Atlantics," Proc. of the TROPEX-72 Interdepartmental Expedition. Leningrad, Gidrometeoizdat, p. 137-149, 1974.

Dmokhovsky, V. I., V. A. Ivanov, "Technique of Aircraft Aerosol Observations," Proc. of MGO, issue 296, p. 87-90, 1973.

Dmokhovsky, V. I., L. S. Ivlev, V. A. Ivanov, "Aircraft Measurements of Atmospheric Aerosol Vertical Structure," Proc. of MGO, issue 276, p. 103-109, 1972.

Ivlev, L. S., "Balloon Investigations of Atmospheric Aerosol Structure," Problems of Atmospheric Physics. Leningrad State University, No. 10, p. 92-103, 1972.

Ivlev, L. S., N. S. Bursakova, S. N. Surikov, "Measurements of Atmospheric Aerosol Distribution in the Surface Layer," Problems of Atmospheric Physics. Leningrad State University, Vol. 6, p. 77-78, 1968.

Ivlev, L. S., V. I. Dmokhovsky, "On the Stability of Aerosol Particles Size Distribution in the Atmospheric Surface Layer," Problems of Atmospheric Physics. Leningrad State University, Vol. 8, p. 52-96, 1970.

Kondratyev, K. Ya., L. S. Ivlev, G. A. Nikolsky, "Results of the Complex Stratospheric Aerosol Research," Metcorology and Hydrology. No. 9, p. 16-26, 1974.

Kondratyev, K. Ya., O. B. Vasilyev, V. S. Grishechkin, L. S. Ivlev, "On Diurnal Variation of Shortwave Spectral Radiative Heat Flux Divergence in the Atmosphere," Reports of the USSR Acad. Sci. Vol. 211, No. 5, p. 1094-1096, 1973.

Pivovarova, Z. I., V. V. Stadnik, "On the Accuracy of Actinometric Network Observational Data and the Optimal Distance Between the Stations," Proc. of MGO, Issue 249, p. 3-32, 1969.

Polevitsky, K. K., E. M. Shadrina, V. N. Adnashkin, "The Field Nephelometer for Automatic Registering Meteorological Visibility," Proc. of MGO, Issue 292, p. 73-85, 1972.

Prokofyev, M. A., N. E. Ter-Markaryants, "Results of Actinometric Measurements in Free Atmosphere in the CAENEX-70 Expedition," Proc. of MGO. Issue 276, p. 43-61, 1972.

Rosen, J. M., "Stratospheric Dust and its Relationship to the Meteoric Influx," Space Science Rev., Vol. 9, No. 9, p. 58-89, 1969.

Sivkov, S. I., "Techniques Used to Determine Solar Radiation Characteristics," Leningrad, Gidrometeoizdat, p. 243, 1968.

Vasilyev, O. B., V. S. Grishechkin, K. Ya. Kondratyev, "Vertical Profiles of Quantative Characteristics of Shortwave Radiation Field in Free Atmosphere," Proc. of MGO, Issue 317, p. 37-47, 1973.

Vinogradova, T. P., V. F. Zhvalev, M. A. Prokofyev, N. E. Ter-Markaryants, N. T. Fedorove, "Radiative Fluxes and Heat Flux Divergences in Free Atmosphere," Proc. of MGO, Issue 296, p. 79-86, 1973.

Zaitseva, N. A., G. N. Kostyanoy, V. I. Shlyakhov, "Mean Multi-year Characteristics of the Longwave Radiation Field in the Free Atmosphere (from the data of the ARZ-network)," Meteorology and Hydrology. No. 7, p. 35-42, 1971.

Zuev, V. E., L. S. Ivlev, K. Ya. Kondratyev, "New Results of Research in Atmospheric Aerosol," Izvestia of the USSR Acad. of Sci. Vol 9, No. 5, 1973.

TABLE 1

SURFACE LAYER AEROSOL SIZE DISTRIBUTION (μm^{-1} cm^{-3})

1500 5 August 1975 - Ryl'sk

	Height (m)			
r(μm)	1	2	5	8
0.22	0.31	-	-	-
0.37	1.216	1.112	0.884	0.398
0.52	0.870	0.059	0.436	0.155
0.62	1.372	1.516	0.968	0.892
0.94	0.139	0.0158	0.173	0.0413
1.00	0.310	0.326	0.484	0.544
1.52	0.0718	0.0158	0.103	0.0413
1.56	0.0877	0.0248	0.0645	0.121
2.18	0.0248	0.111	0.0645	0.0797
2.20	0.00685	0.00495	0.00805	0.0139
2.50	0.0060	0.0106	0.0290	0.0255
3.12	-	0.0124	-	0.0206
3.70	0.00274	0.00322	0.00516	0.00556
4.37	0.0341	0.0218	0.0644	0.0796
6.20	0.0015	0.00148	0.0032	0.0032
12.00	0.0003	0.0006	0.0029	0.0008
$N(>r)$-cm^{-3}				
r=0.2μm	7.90	7.95	3.04	2.50

TABLE 2

AIRCRAFT IMPACTOR MEASURED SIZE DISTRUBUTION (μm^{-1} cm^{-3})

5 August 1975 - Rylsk

	Time and Height (km)							
r(μm)	0640 6.4-7.0	0710 3.65-4.85	0735 4.5-5.8	0805 4.5-5.8	0816 7.0	0845 5.5	0915 2.8	0940 1.35
0.22	6.260	3.340	10.200	6.740	4.120	-	3.540	4.780
0.37	1.810	0.080	1.104	1.316	1.200	1.028	1.064	1.120
0.50	0.684	0.519	0.333	0.336	0.193	0.786	0.996	0.221
0.62	0.232	0.956	0.408	0.540	0.900	0.800	0.904	0.824
0.90	0.0974	0.0329	0.0468	0.0600	0.160	0.137	0.173	0.037
1.00	0.3020	0.1590	0.8160	0.1190	0.2580	0.199	0.276	0.298
1.50	0.0192	0.0212	0.0180	0.0314	0.0576	0.0586	0.0074	0.0098
1.56	0.0356	0.0358	0.0163	0.0400	0.0784	0.1150	0.1090	0.0845
2.00	0.0801	0.0763	0.0076	0.0270	0.0360	0.0458	0.0331	0.0306
2.20	0.0067	0.0143	0.0071	0.0074	0.0026	0.0198	0.0104	0.0044
2.50	0.0062	0.0134	0.0073	0.0151	0.0024	0.0233	0.0146	0.0053
3.10	0.0178	0.0192	0.0038	0.0200	0.0120	0.0576	0.0109	0.0076
3.70	0.0034	0.0040	0.0040	0.0030	0.00072	0.00640	0.00370	0.00107
4.50	0.0245	0.0416	0.0266	0.01700	0.01740	0.0860	0.0218	0.01330
6.20	0.00104	0.00170	0.00290	0.00240	0.00012	0.00360	0.00150	0.00015
12.00	0.0001	0.0024	0.0003	0.0003	0.0001	0.0002	0.0003	0.0003
$N(>r)$-cm^{-3}								
r=0.2 μm	1.46	1.55	3.17	1.46	4.36	0.57	1.80	3.42

TABLE 2 (Continued)

AIRCRAFT IMPACTOR MEASURED SIZE DISTRIBUTION (μm^{-1} cm^{-3})

5 August 1975 - Rylsk

r(μm)	Time and Height (km)							
	0950 0.5	1015 1.35-1.85	1030 2.85	1045 5.5	1106 7.0	1132 2.8-5.5	1147 0.5	1235 7.0
0.22	2.700	6.520	0.876	3.180	6.200	-	-	2.920
0.37	1.692	1.324	1.152	0.956	1.172	0.824	1.080	0.888
0.50	0.864	0.330	0.366	0.900	0.190	1.284	0.606	1.122
0.62	0.708	0.572	0.576	1.184	0.872	0.872	1.356	1.340
0.90	0.0896	0.315	0.0530	0.0768	0.0197	0.2080	0.1200	0.1580
1.00	0.1520	0.111	0.1800	0.1740	0.1270	0.3880	0.3280	0.2800
1.50	0.0432	0.0344	0.0645	0.0320	0.0800	0.0702	0.0554	0.0573
1.56	0.0270	0.0178	0.0461	0.0816	0.0182	0.2560	0.1500	0.1040
2.00	0.0950	0.0178	0.0922	0.0224	0.0094	0.0733	0.0373	0.0435
2.20	0.0101	0.0053	0.0196	0.0105	0.0246	0.0105	0.0084	0.0054
2.50	0.0078	0.0088	0.0124	0.0112	0.0058	0.0106	0.0048	0.0688
3.10	0.0055	0.0058	0.0230	0.0176	0.0047	0.0460	-	0.0130
3.70	0.00590	0.00340	0.00550	0.00480	0.0029	0.00380	0.00320	0.00250
4.50	0.0270	0.0162	0.1040	0.0376	0.0275	0.0322	0.0374	0.0105
6.20	0.00080	0.00120	0.00180	0.00140	0.00104	0.00164	0.00130	0.00100
12.00	0.0002	0.0001	0.0004	0.0002	0.0003	0.0003	0.0003	0.0001
$N(>r)$-cm^{-3}								
r=0.2 μm	2.91	4.46	0.87	1.48	1.43	2.14	2.10	2.26

TABLE 3

AIRCRAFT MEASUREMENTS OF CHEMICAL COMPOSITION

5-6 August 1975 - Rylsk

Date	Height (km)	Element										
		Fe	Mn	Mg	Pb	Cr	Ni	Al	Ca	Cu	Zn	Cd
5 Aug	0.5	44	0.45	4.7	0.15	0.22	0.23	1.1	-	0.77	-	-
5 Aug	7.0	5.5	0.21	1.5	0.09	0.15	0.21	0.6	-	0.56	-	-
5 Aug	5.5	1.5	0.24	2.3	0.13	0.13	0.14	1.2	-	0.43	-	-
5 Aug	2.8	10.0	0.3	1.6	0.21	0.18	0.10	2.2	-	1.19	-	-
5 Aug	1.35	14.0	0.35	2.4	0.33	0.17	0.08	2.5	-	0.30	4.7	-
5 Aug	0.5	25.5	0.62	2.1	0.28	0.31	0.1	8.3	-	1.45	-	<0.01
6 Aug	7.0	-	0.28	-	0.06	0.02	0.15	-	-	0.19	<0.2	-
6 Aug	5.5	3.0	1.25	4.0	-	0.10	-	4.1	-	1.0	<0.2	-
6 Aug	4.8	10.0	2.63	11.7	0.99	0.85	8.66	14.1	8.6	1.96	-	<0.01

TABLE 4

BALLOON IMPACTOR MEASUREMENTS OF AEROSOL CONCENTRATION

August 1975 - Rylsk

Date					
August 1		August 3		August 5	
Height (km)	$N(>r)\text{-}cm^{-3}$ $r=0.2\mu m$	Height (km)	$N(>r)\text{-}cm^{-3}$ $r=0.2\mu m$	Height (km)	$N(>r)\text{-}cm^{-3}$ $r=0.2\mu m$
0	7.03	0		0.05	6.86
0.2	7.95	0.5		0.5	7.30
0.7	6.60	1.0		0.9	2.90
1.2	6.28	1.5		1.4	4.03
1.7	6.46	2.0		1.9	3.94
2.2	5.78	2.5		2.35	4.60
2.7	6.85	3.0		2.85	2.22
3.2	18.5	3.5		3.3	3.67
3.8	13.25	4.0		3.75	6.32
4.3	4.67	4.5		4.2	5.59
4.8	6.54	5.0		4.65	4.36
5.3	5.84	5.5		5.1	4.45
5.8	6.36	6.0		5.65	8.46
6.3	9.00	6.5		6.1	6.00
6.75	7.50	7.00		6.65	3.99
7.2	4.70	7.5		7.1	2.70
7.7	1.65	8.0		7.6	1.16
8.2	1.82	8.5		8.0	0.40
8.7	1.76	9.00		8.4	0.30
9.15	1.50	9.5		8.8	0.20
9.6	1.28	10.00		9.25	0.32
10.1	2.18	10.5		9.7	0.36
10.6	2.05	10.95		10.3	0.80
11.1	0.5	11.4		10.9	0.61
11.6		11.9		11.3	0.90
12.1		12.4		11.8	0.73

NO DATA

TABLE 4 (Continued)

BALLOON IMPACTOR MEASUREMENTS OF AEROSOL CONCENTRATION

August 1975 - Rylsk

Date					
August 1		August 3		August 5	
Height (km)	$N(>r)\text{-}cm^{-3}$ r=0.2 μm	Height (km)	$N(>r)\text{-}cm^{-3}$ r=0.2μm	Height (km)	$N(>r)\text{-}cm^{-3}$ r=0.2μm
12.6		12.9		12.2	0.78
13.1		13.4		12.6	0.43
13.6		13.9		13.05	0.52
14.1		14.4		13.5	0.43
14.6		14.9		14.0	0.48
15.1		15.4		14.5	0.45
15.6		15.9		14.9	0.45
16.1		16.4		15.3	0.49
16.6		16.9		15.8	0.43
17.1		17.4		16.3	0.38
17.6		0.68		16.75	0.42
18.1	0.35	18.4		17.2	0.34
18.6	0.70	18.9		17.7	0.18
19.1	0.50	19.4	0.23	18.2	0.14
19.6	0.37	19.85	0.23	18.7	0.10
20.1	0.36	20.3	0.31	19.2	0.10
20.6	0.37	20.8	0.25	19.7	-
21.1	0.46	21.8	0.17	20.2	-
21.6	0.275	22.3	0.24	20.65	-
22.1	0.26	22.8	0.48	21.1	-
22.6	0.314	23.3	0.52	21.55	-
23.1	0.28	23.8	0.50	22.0	-
23.6	0.20	24.3	0.54	22.45	-
24.1	0.10	24.8	0.42	22.9	-
24.6	0.05	25.3	0.34		
25.1	0.05	25.8	0.32		

NO DATA

NO DATA

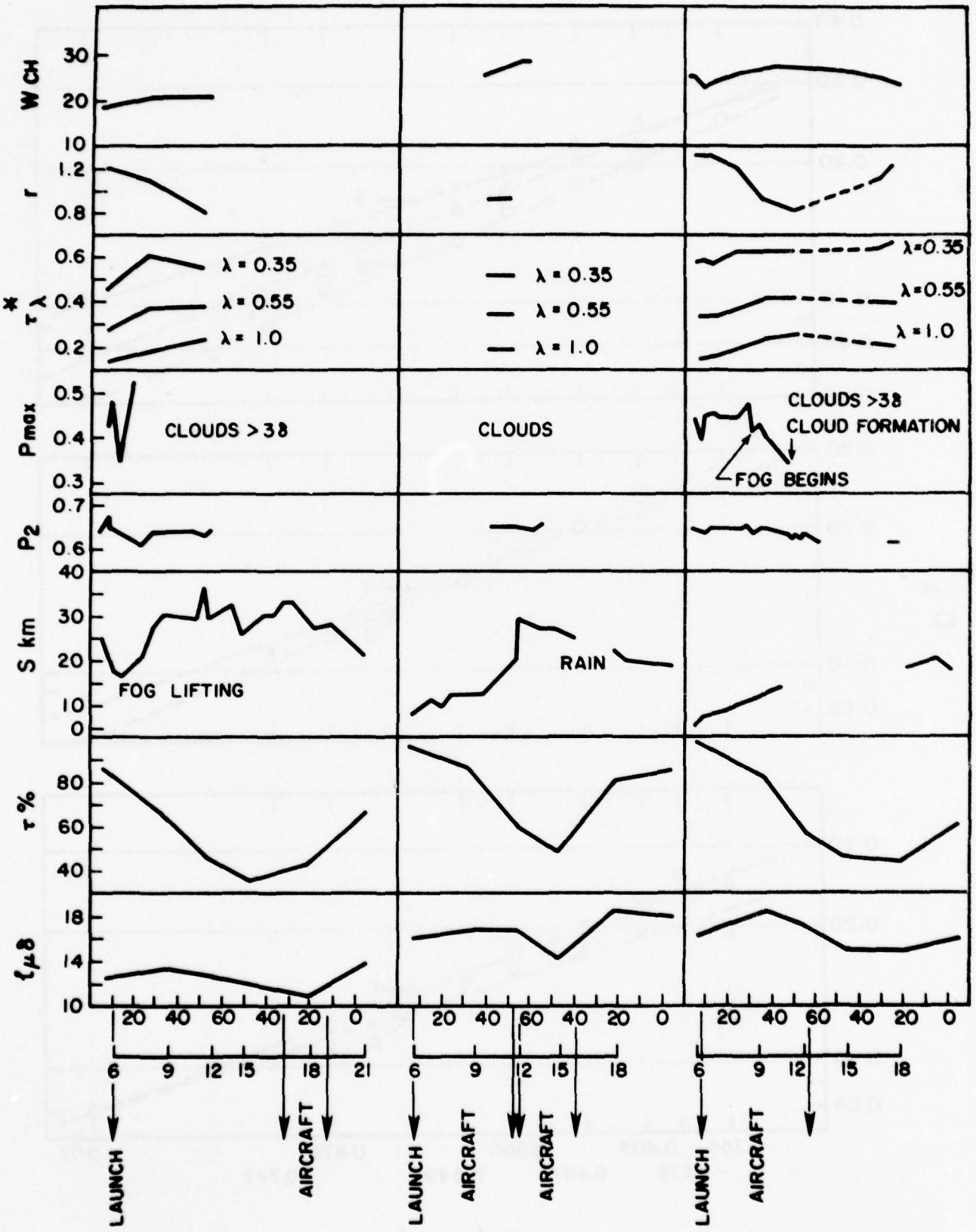
W CH
r
τ λ
λ = 0.35
λ = 0.55
λ = 1.0
Pmax
CLOUDS >38
CLOUDS
CLOUDS >38
CLOUD FORMATION
FOG BEGINS
P2
S km
FOG LIFTING
RAIN
τ %
ℓμ8
LAUNCH
AIRCRAFT
AIRCRAFT
LAUNCH
AIRCRAFT
LAUNCH
AIRCRAFT

FIGURE 1

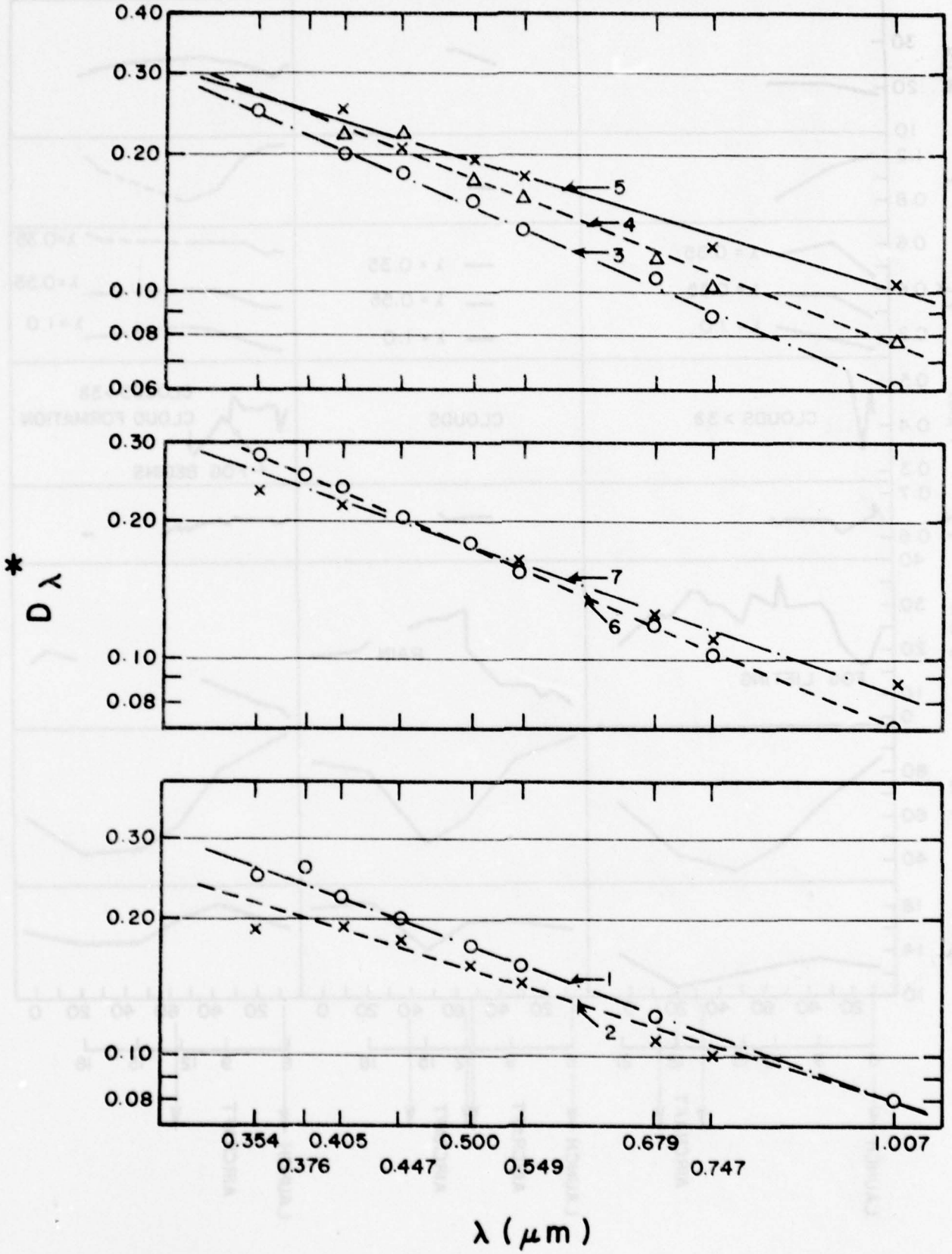
0.40
0.30
0.20
0.10
0.08
0.06
5
4
3
0.30
0.20
0.10
0.08
7
6
0.30
0.20
0.10
0.08
1
2
0.354
0.376
0.405
0.447
0.500
0.549
0.679
0.747
1.007
D^*_λ
λ (μm)

FIGURE 2

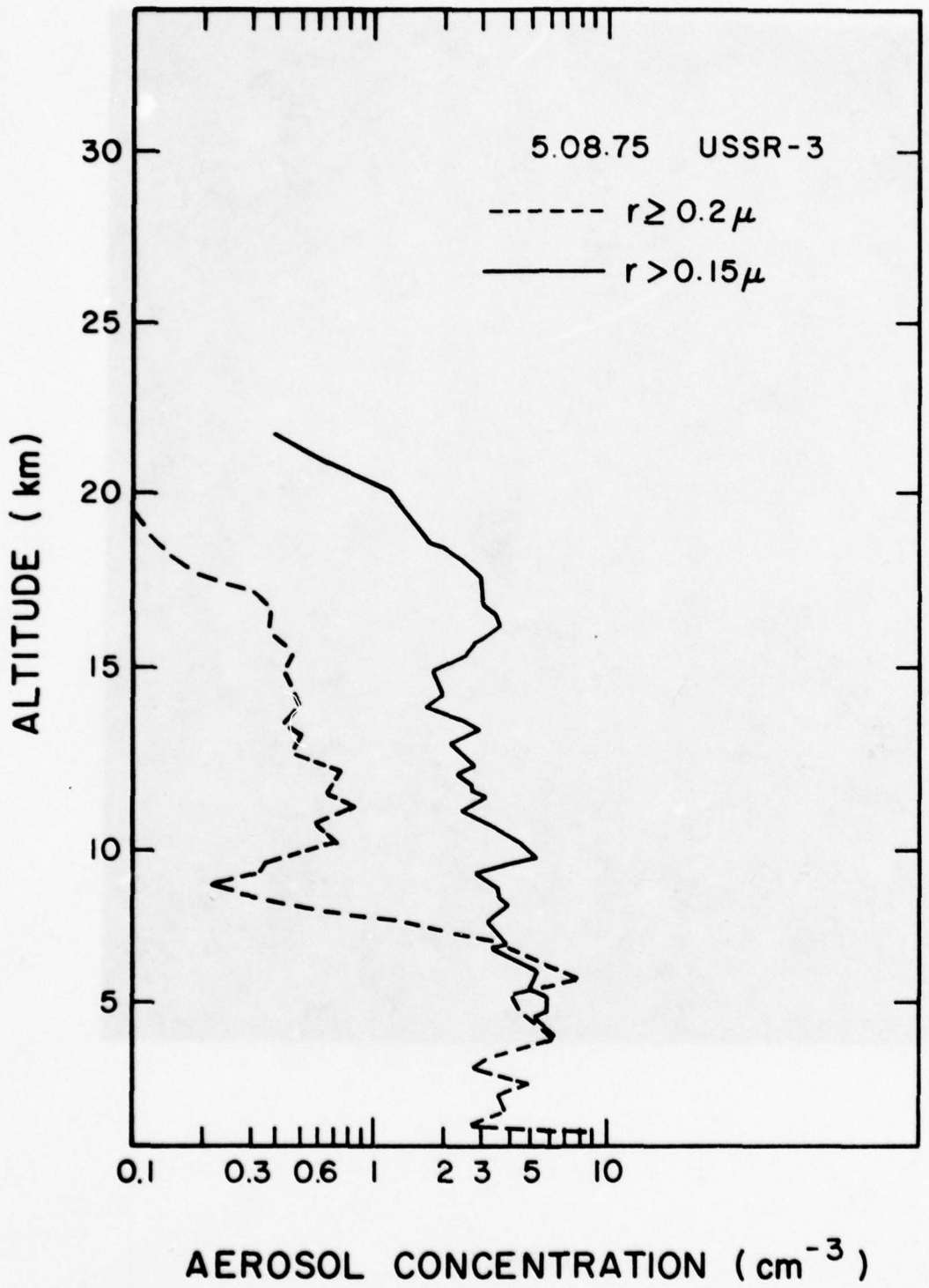
5.08.75 USSR-3
r≥0.2μ
r>0.15μ
ALTITUDE (km)
30
25
20
15
10
5
0.1
0.3
0.6
1
2
3
5
10
AEROSOL CONCENTRATION (cm⁻³)

FIGURE 3

FIGURE 4

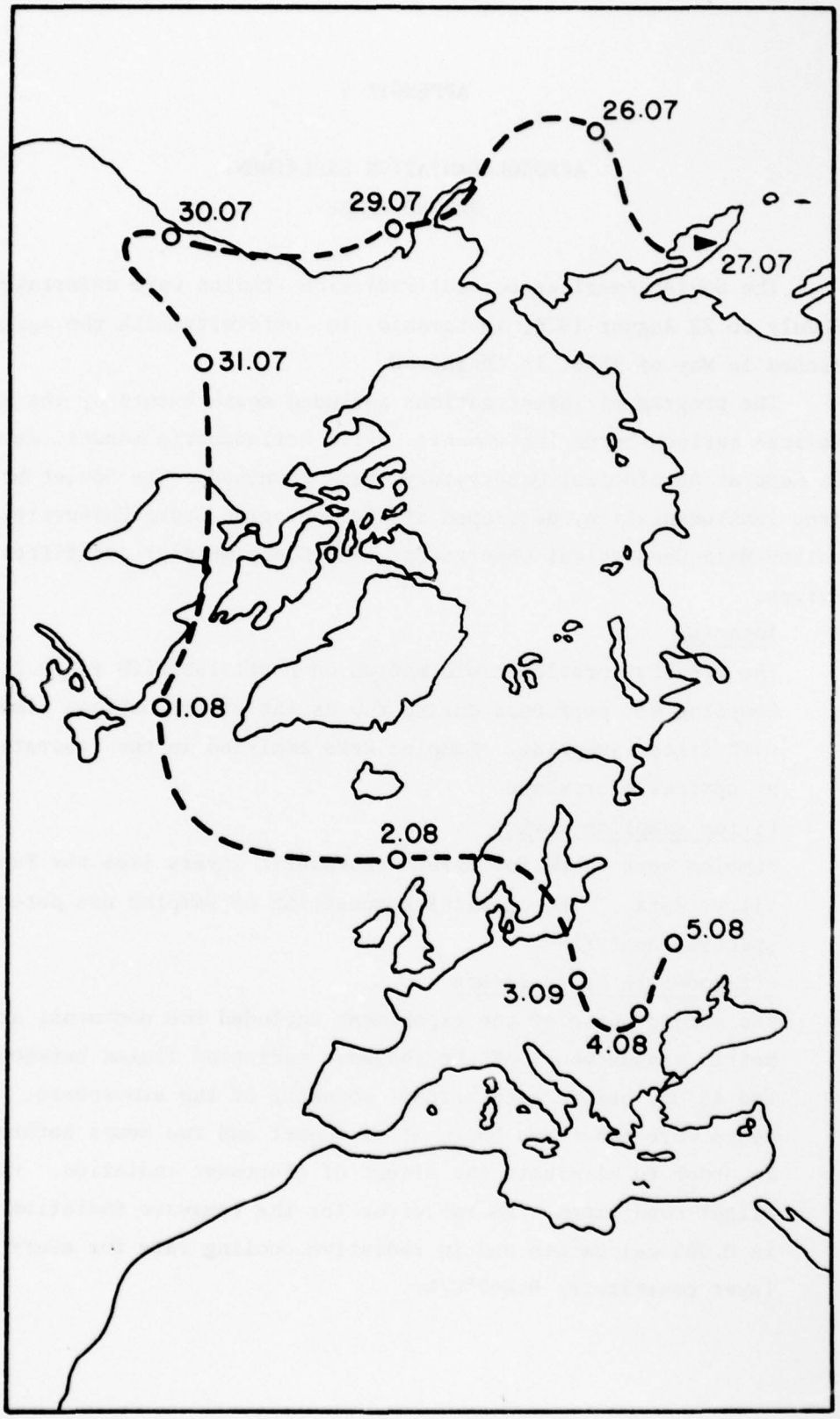

FIGURE 5

APPENDIX 5

AEROSOL-RADIATION EXPERIMENT
SECOND PHASE

The Soviet-American aerosol-radiation studies were undertaken from 25 July to 22 August 1976, in Laramie, in conformity with the agreement reached in May of 1976, in Leningrad.

The program of investigations included measurements by the Soviet and American balloon-borne instruments. Five actinometric sondes, developed in the Central Aerological Observatory, were launched. The Soviet balloon-borne instrumentation, developed at the Leningrad State University and the Voeikov Main Geophysical Observatory, included impactor and filter sampling devices.

Impactor

The impactor provides information on particles with $r \geq 0.2$ μm. Sampling was performed during the ascent of the balloon simultaneously with filter sampling. Samples were analyzed in the laboratory using an optical microscope.

Filter sampling device

Samples were taken for three atmospheric layers (see the Table of filter data). The chemical composition of samples was determined by spectral analysis.

Actinometric measurements

The second phase of the experiment included the nocturnal actinometric measurements of the longwave radiation fluxes between 4 μm and 40 μm, before each aerosol sounding of the atmosphere. Measurements were taken two hours after sunset and two hours before sunrise in order to eliminate the effect of shortwave radiation. For actual flight conditions, the rms error for the longwave radiation fluxes is 0.005 cal/cm^{2}min and in radiative cooling rate for every 100 mb layer constitutes 0.007°C/hr.

Evaluation of the impact of various factors on the rate of radiative temperature variation is greatly facilitated by the availability of spectral measurement data; whereas, in actinometric (integral) soundings, the results of accompanying aerological measurements are of particular importance, i.e., data on the content of water vapor, aerosol, ozone and other active gaseous components in the atmosphere, such as carbon dioxide, freons, etc. The data, when used for numerical modeling, make it possible to quantitatively evaluate the effect of aerosol and other factors on the longwave radiation transfer.

The following table lists data on actinometric radiometersonde launches. All of them were carried out in clear sky (20-30% cloudiness) and weak wind conditions.

DATA ON ACTINOMETRIC RADIOMETERSONDE LAUNCHES

Flt. No.	Date	Time (MST)	Temperature °C		Pressure (mb)	Maximum Height And Time When Reached	
			Wet	Dry		Height (km)	Time
W-126	31 July	0402	15.8	18.2	784.0	22.35	0526
W-128	3 Aug.	2258	13.5	16.8	784.6	25.09	0033
W-129	4 Aug.	0358	10.2	13.8	784.5	28.26	0527
W-131	5 Aug.	2241	13.8	18.2	784.6	29.47	0041
W-132	6 Aug.	0412	12.1	14.9	784.6	26.65	0551

All the results obtained by the Soviet side are presented in tables and graphs in this appendix. Symbols used for measured quantities in tables and graphs are as follows.

...$e^{\downarrow}$	Downward longwave radiation flux.
-- t_b	Temperature
- . - F	Effective longwave radiation flux.
- .. - $e\uparrow$	Upward longwave radiation flux.
$\partial T/\partial \tau$	Rate of radiative change of temperature.

W-126

July 31, 1976

Laramie, Wyoming

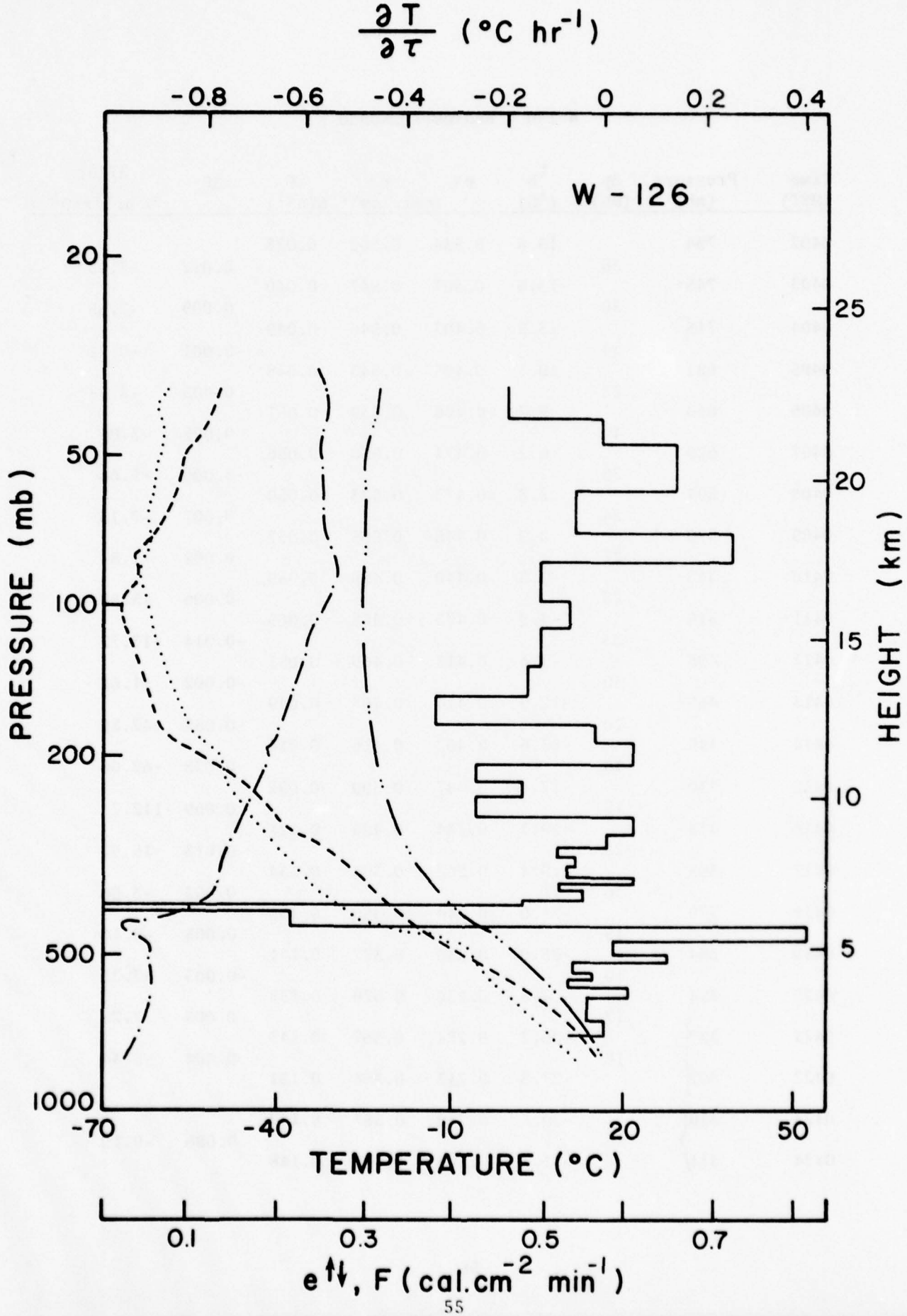
$\frac{\partial T}{\partial \tau}$ (°C hr^{-1})
-0.8
-0.6
-0.4
-0.2
0
0.2
0.4
W - 126
20
50
100
200
500
1000
PRESSURE (mb)
25
20
15
10
5
HEIGHT (km)
-70
-40
-10
20
50
TEMPERATURE (°C)
0.1
0.3
0.5
0.7
e↑↓, F (cal.cm^{-2} min^{-1})

W-126 - Radiometersonde

Time (MST)	Pressure (mb)	Δp (mb)	t_b (°C)	e↓	e↑ (cal. cm^{-2} min^{-1})	F	ΔF	$\partial T/\partial \tau$ °C hr^{-1} x10^2
0402	784		13.8	0.534	0.562	0.028		
		39					0.012	-7.53
0403	745		13.6	0.507	0.547	0.040		
		30					0.009	-7.35
0404	715		13.5	0.407	0.546	0.049		
		34					-0.001	+0.71
0405	681		10.7	0.495	0.543	0.048		
		21					0.003	-3.48
0406	660		9.7	0.488	0.539	0.051		
		40					0.005	-3.06
0407	620		6.2	0.474	0.530	0.056		
		26					-0.006	+5.64
0408	594		2.8	0.473	0.523	0.050		
		24					0.007	-7.13
0409	570		0.2	0.448	0.505	0.057		
		27					0.002	-1.81
0410	543		-2.5	0.440	0.499	0.059		
		25					0.006	-5.88
0411	518		-4.9	0.423	0.488	0.065		
		23					-0.014	+13.72
0412	495		-7.6	0.418	0.469	0.051		
		30					-0.002	+1.62
0413	465		-12.9	0.414	0.463	0.049		
		20					-0.035	+42.88
0414	445		-13.6	0.402	0.416	0.014		
		15					0.038	-62.06
0415	430		-17.4	0.347	0.399	0.052		
		15					0.069	-112.7
0416	415		-19.1	0.284	0.405	0.121		
		20					0.013	-15.92
0417	395		-19.4	0.262	0.396	0.134		
		16					0.002	-3.06
0418	379		-21.0	0.244	0.380	0.136		
		15					0.005	-8.16
0419	364		-23.0	0.236	0.377	0.141		
		10					-0.003	+7.35
0420	354		-24.8	0.232	0.370	0.138		
		17					0.005	-7.20
0421	337		-26.2	0.224	0.367	0.143		
		18					0.004	-5.44
0422	332		-27.8	0.213	0.364	0.151		
0423	319		-29.5	0.210	0.357	0.147		
		16					0.006	-9.19
0424	311		-31.1	0.204	0.352	0.148		

W-126 - Radiometersonde (Continued)

Time (MST)	Pressure (mb)	Δp (mb)	t_b (°C)	e↓	e↑ (cal. cm^{-2} min^{-1})	F	ΔF	∂T/∂τ °C hr^{-1} x 10^2
0425	303	20	-32.8	0.195	0.348	0.153	-0.001	+1.22
0426	299		-34.5	0.194	0.343	0.149		
0427	283	17	-36.7	0.185	0.337	0.152	-0.005	+7.2
0428	273		-38.4	0.182	0.334	0.152		
0429	266	20	-40.5	0.179	0.326	0.147	0.021	-25.72
0430	256		-42.0	0.159	0.320	0.161		
0431	246		-44.1	0.148	0.316	0.168		
0432	233	18	-45.4	0.140	0.313	0.173	0.012	-16.32
0433	233		-46.7	0.130	0.309	0.179		
0434	228	19	-48.6	0.128	0.308	0.180	0.020	-25.77
0435	218		-50.6	0.121	0.321	0.200		
0436	209		-51.8	0.118	0.318	0.200		
0437	203	18	-52.7	0.113	0.303	0.190	0.005	+6.79
0438	198		-54.1	0.109	0.301	0.192		
0439	191		-55.8	0.105	0.300	0.195		
0440	186	19	-58.8	0.105	0.304	0.199	0.001	-1.27
0441	179		-60.2	0.097	0.303	0.206		
0442	172		-62.5	0.097	0.293	0.196		
0443	164	19	-63.7	0.086	0.297	0.211	0.027	-34.81
0444	158		-64.3	0.086	0.297	0.211		
0445	153		-63.5	0.073	0.296	0.223		
0446	148	19	-63.9	0.068	0.298	0.230	0.012	-15.46
0447	142		-65.5	0.063	0.299	0.236		

W-126 - Radiometersonde (Continued)

Time (MST)	Pressure (mb)	Δp (mb)	t_b (°C)	e↓	e↑ (cal. cm^{-2} min^{-1})	F	ΔF	∂T/∂τ °C hr^{-1} x 10^2
0448	134		-67.5	0.068	0.303	0.235		
0449	129		-67.0	0.057	0.304	0.247		
		21					0.011	-12.81
0450	124		-65.5	0.052	0.297	0.245		
0451	118		-64.6	0.054	0.293	0.239		
0452	113		-66.6	0.052	0.298	0.246		
0453	108		-67.0	0.057	0.295	0.238		
		15					0.004	-6.52
0454	103		-67.7	0.049	0.295	0.246		
0455	98		-67.6	0.049	0.299	0.250		
0456	94		-67.0	0.041	0.299	0.258		
0457	90		-65.4	0.036	0.298	0.262		
		17					0.009	-12.96
0458	87		-65.2	0.043	0.296	0.253		
0459	84		-66.1	0.038	0.300	0.262		
0500	81		-65.6	0.040	0.299	0.259		
0501	79		-63.5	0.041	0.297	0.256		
0502	75		-62.3	0.047	0.292	0.245		
		10					-0.011	+26.96
0503	73		-60.8	0.042	0.293	0.251		
0504	71		-61.0	0.044	0.292	0.248		
0505	68		-60.7	0.047	0.291	0.244		
		12					0.003	-6.12
0506	66		-59.6	0.046	0.294	0.248		
0507	64		-58.0	0.048	0.290	0.242		
0508	61		58.5	0.050	0.293	0.243		
0509	59		-58.5	0.048	0.299	0.251		
0510	56		-58.9	0.049	0.300	0.251		

W-126 - Radiometersonde (Continued)

Time (MST)	Pressure (mb)	Δp (mb)	t_b (°C)	e↓	e↑ (cal. cm^{-2}	F min^{-1})	ΔF	∂T/∂τ °C hr^{-1} x 10^2
0511	55	12	-58.2	0.055	0.298	0.243	-0.007	+14.28
0512	53		-57.9	0.055	0.297	0.242		
0513	51		-57.0	0.055	0.295	0.240		
0514	49		-54.8	0.050	0.295	0.245		
0515	48		-55.0	0.050	0.299	0.249		
0516	47	5	-55.0	0.057	0.301	0.244	0.00	0.00
0517	46		-54.7	0.054	0.300	0.246		
0518	44		-53.8	0.058	0.302	0.244		
0519	42	5	-52.7	0.058	0.302	0.244	-.002	-19.60
0520	40		-52.0	0.054	0.309	0.255		
0521	39		-51.7	0.057	0.305	0.248		
0522	38		-51.7	0.057	0.305	0.248		
05.23	37		-51.8	0.059	0.307	0.248		

W-127

July 31, 1976

Laramie, Wyoming

W-127 - Filter Samples

Concentration ($\mu g/m^3$)

Height (km)	Element									
	Mg	Al	Ca	Ni	Cr	Cu	Pb	Mn	Fe	Zn
6.1 - 10.15	<0.3	0.1	0.4	≤0.2	<0.02	0.03	≤0.03	<0.004	≤0.3	<0.6
10.15 - 15.0	1.8	0.2	2.0	≤0.2	<0.02	>0.7	≤0.03	0.14	2.0	<0.6
15.0 - 23.35	2.7	0.3	2.0	<0.2	0.08	0.5	<0.03	0.2	≥6.6	≤0.6

W-128

August 3, 1976

Laramie, Wyoming

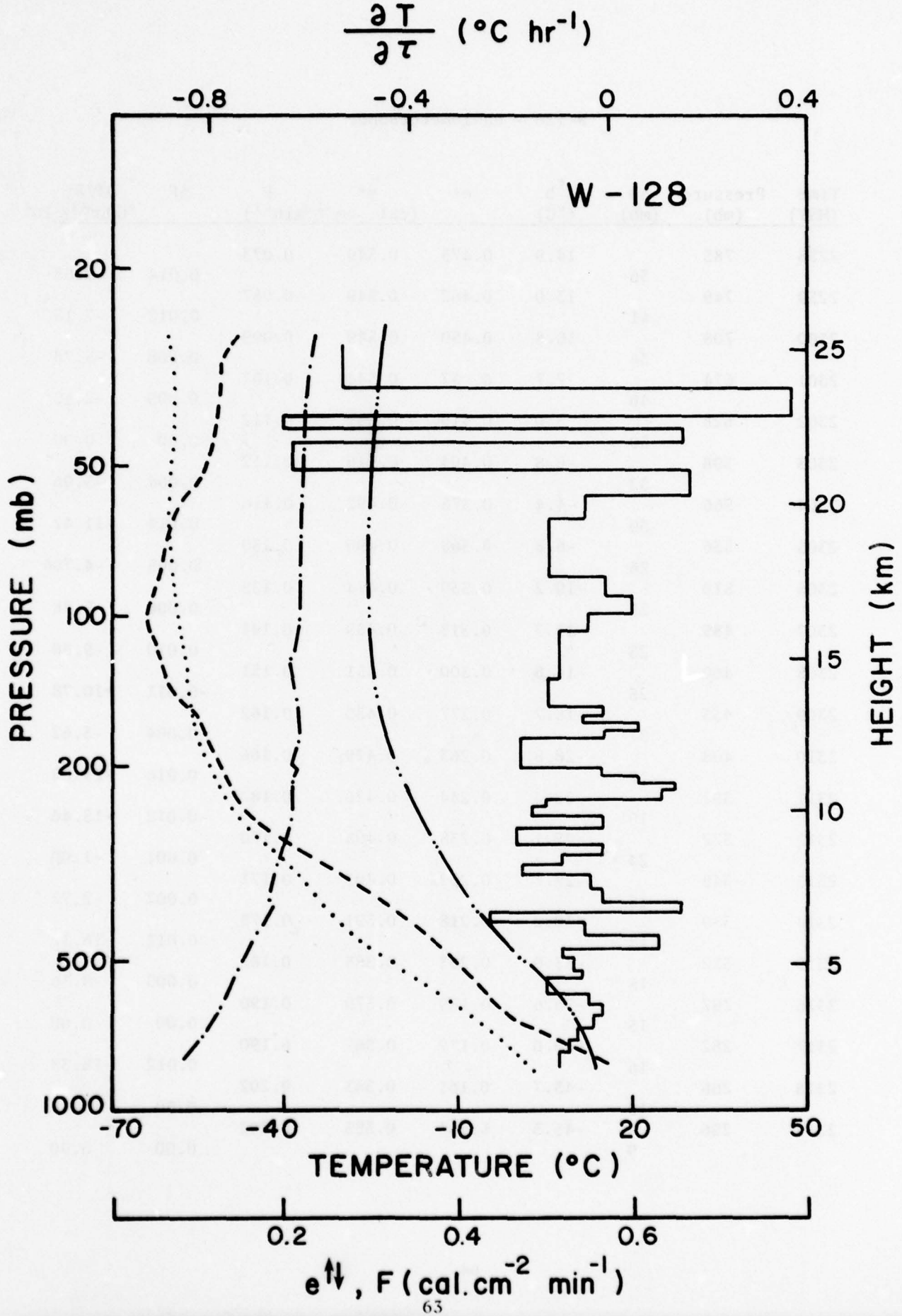
$\frac{\partial T}{\partial \tau}$ (°C hr^{-1})
-0.8
-0.4
0
0.4
W - 128
20
50
100
200
500
1000
PRESSURE (mb)
25
20
15
10
5
HEIGHT (km)
-70
-40
-10
20
50
TEMPERATURE (°C)
0.2
0.4
0.6
e$^{\uparrow\downarrow}$, F (cal.cm^{-2} min^{-1})

W-128 - Radiometersonde

Time (MST)	Pressure (mb)	Δp (mb)	t_b (°C)	e↓	e↑ (cal. cm^{-2} min^{-1})	F	ΔF	∂T/∂τ °C hr^{-1} x 10^2
2258	785		14.9	0.475	0.549	0.073		
		36					0.014	-9.63
2259	749		13.0	0.462	0.549	0.087		
		41					0.012	-7.15
2300	708		10.8	0.450	0.549	0.099		
		34					0.008	-5.76
2301	674		7.7	0.437	0.544	0.107		
		46					0.005	-2.65
2302	628		3.0	0.419	0.531	0.112		
		30					0.00	0.00
2303	598		-0.8	0.404	0.516	0.112		
		32					0.004	-3.06
2304	566		-4.4	0.376	0.492	0.116		
		30					0.014	-11.42
2305	536		-6.8	0.360	0.490	0.130		
		26					0.005	-4.704
2306	510		-10.2	0.339	0.474	0.135		
		25					0.006	-5.88
2307	485		-11.7	0.318	0.459	0.141		
		25					0.010	-9.80
2308	460		-14.8	0.300	0.451	0.151		
		25					-0.011	+10.78
2309	435		-18.7	0.277	0.439	0.162		
		27					0.004	-3.62
2310	408		-20.8	0.263	0.429	0.166		
		17					0.016	-23.05
2311	391		-22.4	0.244	0.426	0.182		
		19					-0.012	+15.46
2312	372		-25.1	0.238	0.408	0.170		
		24					0.001	-1.00
2313	348		-27.7	0.232	0.403	0.171		
		18					0.002	-2.72
2314	330		-30.2	0.218	0.391	0.173		
		18					0.012	-16.32
2315	312		-33.9	0.203	0.388	0.185		
		15					0.005	-8.16
2316	297		-36.6	0.189	0.379	0.190		
		15					0.00	0.00
2317	282		-40.0	0.177	0.367	0.190		
		16					0.012	-18.38
2318	266		-43.7	0.161	0.363	0.202		
		10					0.00	0.00
2319	256		-45.5	0.153	0.355	0.202		
		9					0.00	0.00

W-128 - Radiometersonde (Continued)

Time (MST)	Pressure (mb)	Δp (mb)	t_b (°C)	e↓	e↑ (cal. cm^{-2}	F min^{-1})	ΔF	∂T/∂τ °C hr^{-1} x 10^2
2320	247		-47.4	0.145	0.347	0.202		
		10					0.006	-14.70
2321	237		-48.8	0.134	0.342	0.208		
		8					0.004	-12.25
2322	229		-49.9	0.125	0.337	0.212		
		12					-0.006	+12.25
2323	217		-51.0	0.122	0.328	0.206		
		5					-0.003	+14.7
2324	212		-51.2	0.118	0.321	0.203		
		11					-0.003	+6.66
2325	201		-52.3	0.115	0.315	0.200		
		9					0.00	0.00
2326	192		-54.0	0.114	0.314	0.200		
2327	185		-55.4	0.111	0.312	0.201		
		20					0.014	-17.15
2328	178		-54.9	0.097	0.309	0.212		
2329	172		-54.4	0.094	0.308	0.214		
		6					0.0	0.0
2330	166		-55.2	0.093	0.307	0.214		
		7					-0.002	+6.98
2331	159		-55.4	0.093	0.305	0.212		
		6					0.001	-4.07
2332	153		-56.6	0.092	0.305	0.213		
		6					0.0	0.0
2333	147		-57.2	0.092	0.305	0.213		
2334	140		-58.8	0.092	0.300	0.208		
		13					0.006	-11.30
2335	134		-57.9	0.092	0.299	0.207		
		5					0.0	0.0
2336	129		-61.1	0.092	0.299	0.207		
2337	123		-63.1	0.089	0.299	0.210		
2338	118		-62.7	0.084	0.297	0.213		
		20					0.011	-9.05
2339	113		-62.5	0.081	0.296	0.215		
2340	109		-61.9	0.076	0.294	0.218		
2341	104		-63.6	0.076	0.294	0.218		
		7					0.001	-3.48

W-128 - Radiometersonde (Continued)

Time (MST)	Pressure (mb)	Δp (mb)	t_b (°C)	e↓	e↑ (cal. cm^{-2} min^{-1})	F	ΔF	$\partial T/\partial \tau$ °C hr^{-1} x 10^2
2342	100		-63.2	0.075	0.294	0.219		
2343	97	9	-63.7	0.075	0.294	0.219	-0.002	+5.44
2344	91		-62.2	0.073	0.290	0.217		
2345	88	7	-61.1	0.072	0.289	0.217	0.00	0.00
2346	82		-61.4	0.074	0.291	0.217		
2347	81		-61.4	0.074	0.291	0.217		
2348	77		-61.4	0.070	0.291	0.221		
2349	74	19	-61.8	0.074	0.295	0.221	0.009	-11.60
2350	71		-61.1	0.068	0.291	0.223		
2351	69		-61.3	0.071	0.295	0.224		
2352	65		-60.2	0.066	0.291	0.225		
2353	62		-59.2	0.067	0.293	0.226		
2354	60	6	-58.5	0.067	0.293	0.226	0.001	-4.07
2355	58		-57.6	0.066	0.293	0.227		
2356	56		-56.7	0.066	0.293	0.227		
2357	54	7	-55.6	0.066	0.292	0.226	-0.005	+17.49
2358	52		-53.8	0.068	0.292	0.224		
2359	49	5	-53.5	0.070	0.292	0.222	0.013	-63.70
0000	47		-52.1	0.065	0.290	0.225		
0001	46		-51.4	0.068	0.297	0.229		
0002	44	3	-50.0	0.066	0.301	0.235	0.02	+16.33
0003	43		-50.4	0.073	0.303	0.230		

W-128 - Radiometersonde (Continued)

Time (MST)	Pressure (mb)	Δp (mb)	t_b (°C)	e↓	e↑ (cal. cm^{-2} min^{-1})	F	ΔF	$\partial T/\partial \tau$ °C hr^{-1} x 10^2
0004	41		-51.2	0.073	0.306	0.233		
0005	39	2	-52.3	0.073	0.311	0.238	0.005	-64.25
0006	37		-52.8	0.080	0.313	0.233		
		5					-0.008	+39.2
0007	36		-52.0	0.079	0.307	0.228		
0008	34		-52.8	0.077	0.307	0.230		
0009	33		-52.1	0.074	0.310	0.236		
		6					0.013	-53.07
0010	32		-52.0	0.074	0.310	0.236		
0011	31		-51.4	0.073	0.310	0.237		
0012	29		-49.4	0.069	0.310	0.241		
0013	28		-48.5	0.067	0.310	0.243		

W-129

August 4, 1976

Laramie, Wyoming

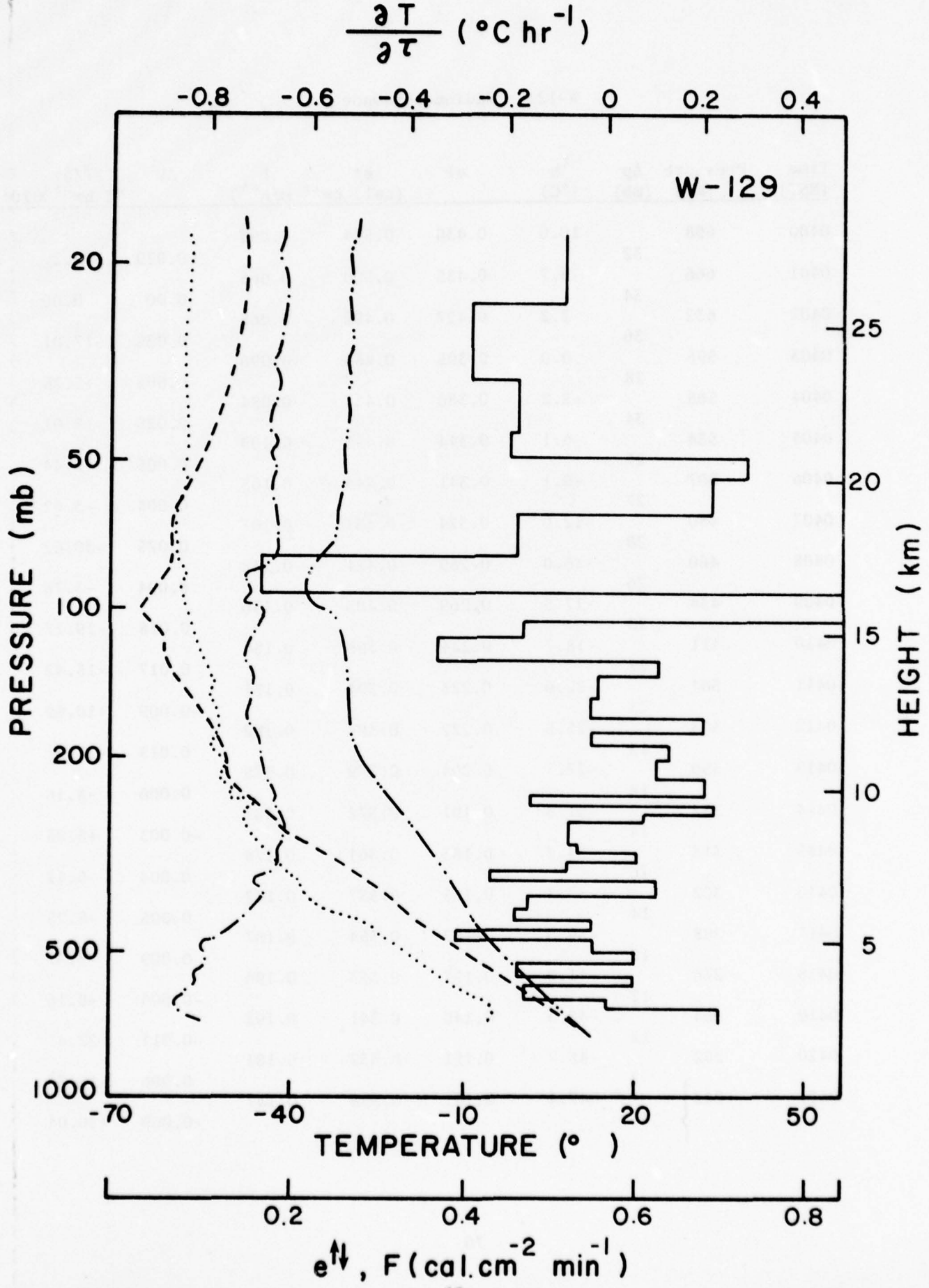
$\frac{\partial T}{\partial \tau}$ (°C hr^{-1})
-0.8
-0.6
-0.4
-0.2
0
0.2
0.4
W-129
PRESSURE (mb)
20
50
100
200
500
1000
HEIGHT (km)
25
20
15
10
5
-70
-40
-10
20
50
TEMPERATURE (°)
0.2
0.4
0.6
0.8
$e^{\uparrow\downarrow}$, F (cal.cm^{-2} min^{-1})

W-129 - Radiometersonde

Time (MST)	Pressure (mb)	Δp (mb)	t_b (°C)	e↓	e↑ (cal. cm^{-2} min^{-1})	F	ΔF	$\partial T/\partial \tau$ °C hr^{-1} x 10^2
0400	698		10.0	0.430	0.524	0.094		
		32					-0.029	+22.2
0401	666		6.7	0.435	0.500	0.065		
		34					0.00	0.00
0402	632		3.2	0.427	0.492	0.065		
		36					0.025	-17.01
0403	596		0.0	0.395	0.485	0.090		
		28					-0.006	+5.25
0404	568		-3.2	0.380	0.464	0.084		
		34					0.025	-18.01
0405	534		-6.1	0.344	0.453	0.109		
		27					-0.006	+5.44
0406	507		-9.1	0.341	0.444	0.103		
		27					0.004	-3.62
0407	480		-12.0	0.324	0.431	0.107		
		20					0.025	-30.62
0408	460		-16.0	0.289	0.421	0.132		
		26					0.004	-3.76
0409	434		-17.5	0.269	0.405	0.136		
		23					0.018	-19.17
0410	411		-18.7	0.244	0.398	0.154		
		27					0.017	-15.42
0411	384		-22.6	0.223	0.394	0.171		
		21					-0.009	+10.50
0412	363		-25.5	0.222	0.384	0.162		
		13					0.013	-24.5
0413	350		-27.7	0.204	0.379	0.175		
		18					0.006	-8.16
0414	332		-31.5	0.191	0.372	0.181		
		14					-0.003	+5.25
0415	318		-34.3	0.183	0.361	0.178		
		16					0.004	-6.12
0416	302		-37.3	0.175	0.357	0.182		
		14					0.005	-8.75
0417	288		-39.3	0.167	0.354	0.187		
		12					0.009	-8.37
0418	276		-41.0	0.157	0.353	0.196		
		12					-0.004	+8.16
0418	264		-43.3	0.149	0.341	0.192		
		12					-0.011	+22.45
0420	252		-45.7	0.151	0.332	0.181		
		9					0.006	-16.33
0421	243	11	-47.4	0.141	0.328	0.187	-0.009	+20.04

W-129 - Radiometersonde (Continued)

Time (MST)	Pressure (mb)	Δp (mb)	t_b (°C)	e↓	e↑ (cal. cm^{-2} min^{-1})	F	ΔF	$\partial T/\partial \tau$ °C hr^{-1} x 10^2
0422	232	17	-48.8	0.137	0.315	0.178	-0.014	+20.17
0423	226		-50.5	0.132	0.305	0.173		
0424	218	17	-50.5	0.126	0.299	0.173	-0.007	+10.08
0425	209		-50.0	0.124	0.290	0.166		
0426	201	14	-50.2	0.121	0.280	0.159	-0.007	+12.25
0427	195		-50.3	0.119	0.278	0.159		
0428	188	15	-50.9	0.111	0.276	0.165	+0.002	-3.26
0429	180		-52.6	0.112	0.273	0.161		
0430	174	14	-52.9	0.116	0.264	0.148	-0.011	+19.25
0431	166		-54.8	0.112	0.262	0.150		
0432	159	14	-55.6	0.111	0.260	0.149	0.002	-3.55
0433	155		-56.3	0.108	0.260	0.152		
0434	146	13	-58.4	0.111	0.264	0.153	0.001	-1.88
0435	139		-58.9	0.106	0.259	0.153		
0436	132	12	-59.8	0.106	0.259	0.153	-0.005	+10.2
0437	127		-60.0	0.105	0.253	0.148		
0438	123	10	-61.0	0.100	0.256	0.156	0.014	-34.3
0439	117		-61.4	0.095	0.257	0.162		
0440	112	10	-61.6	0.092	0.257	0.165	0.007	-17.15
0441	107		-62.5	0.089	0.258	0.169		
0442	103	14	-63.7	0.085	0.259	0.174	-0.026	+45.5
0443	100		-65.3	0.085	0.228	0.143		

W-129 - Radiometersonde (Continued)

Time (MST)	Pressure (mb)	Δp (mb)	t_b (°C)	e ↓	e↑ (cal. cm^{-2}	F min^{-1})	ΔF	∂T/∂τ °C hr^{-1} x 10^2
0444	93		-65.1	0.080	0.223	0.143		
0445	89		-62.3	0.075	0.223	0.148		
0446	86		-62.0	0.079	0.221	0.142		
		14					0.040	-70.0
0447	82		-61.5	0.072	0.255	0.183		
0448	79		-61.3	0.073	0.256	0.183		
0449	77		-59.7	0.068	0.254	0.186		
0450	74		-60.4	0.069	0.259	0.190		
		14					0.010	-17.5
0451	70		-60.4	0.072	0.261	0.189		
0452	67		-59.6	0.071	0.259	0.188		
0453	65		-59.6	0.072	0.265	0.193		
0454	62		-57.8	0.081	0.262	0.181		
0455	59		-56.0	0.081	0.263	0.182		
		11					-0.010	+22.27
0456	56		-56.0	0.085	0.265	0.180		
0457	54		-55.3	0.083	0.266	0.183		
0458	52		-54.5	0.080	0.266	0.186		
		5					-0.006	+29.4
0459	49		-54.4	0.089	0.266	0.177		
0500	48		-54.6	0.089	0.269	0.180		
0501	46		-54.1	0.087	0.271	0.184		
		5					0.004	-19.6
0502	44		-53.3	0.088	0.269	0.181		
0503	42		-52.7	0.086	0.273	0.187		
0504	40		-52.7	0.087	0.273	0.186		
0505	39		-52.4	0.085	0.274	0.189		
		10					0.007	-17.15
0506	37		-51.0	0.083	0.275	0.192		

W-129 - Radiometersonde (Continued)

Time (MST)	Pressure (mb)	Δp (mb)	t_b (°C)	e↓	e↑ (cal. cm^{-2}	F min^{-1})	ΔF	∂T/∂τ °C hr^{-1} x 10^2
0507	35		-50.8	0.086	0.282	0.196		
0508	34		-49.6	0.085	0.273	0.188		
0509	33		-49.2	0.085	0.272	0.187		
0510	32		-48.9	0.085	0.278	0.193		
0511	30		-49.6	0.085	0.283	0.198		
0512	28	10	-49.6	0.085	0.281	0.196	0.011	-26.95
0513	27		-49.3	0.084	0.282	0.198		
0514	26		-48.5	0.084	0.281	0.197		
0515	25		-47.3	0.081	0.280	0.199		
0516	24		-47.1	0.082	0.281	0.199		
0517	23		-47.3	0.083	0.284	0.201		
0518	22		-48.1	0.082	0.284	0.202		
0519	21	7	-47.0	0.079	0.283	0.204	0.002	-7.00
0520	20		-46.1	0.080	0.281	0.201		
0521	19		-46.1	0.083	0.280	0.197		
0522	18		-46.6	0.084	0.281	0.197		
0523	17		-47.0	0.082	0.283	0.201		

W-130

August 4, 1976

Laramie, Wyoming

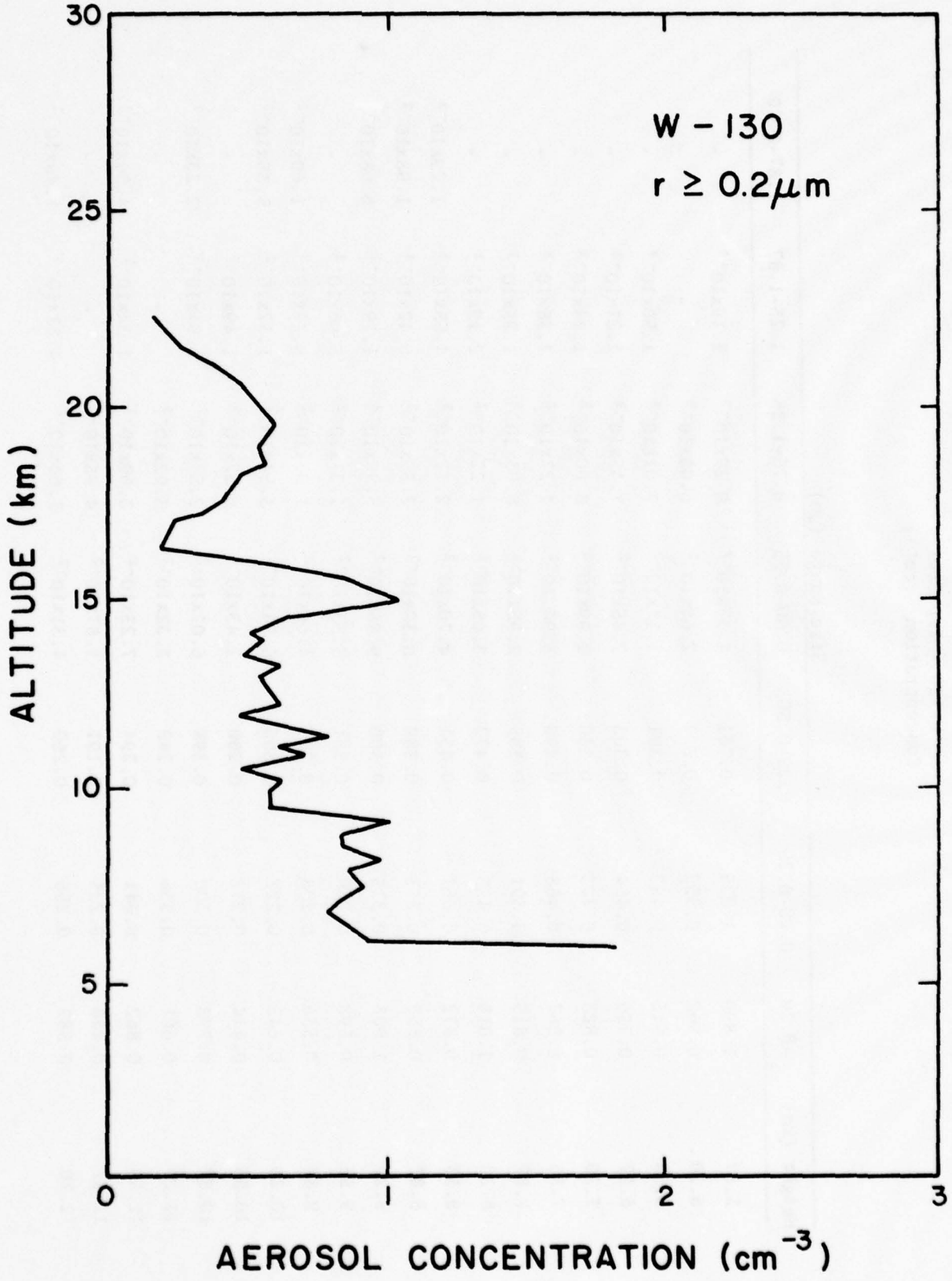
W - 130
r ≥ 0.2μm
30
25
20
15
10
5
0
1
2
3
ALTITUDE (km)
AEROSOL CONCENTRATION (cm^{-3})

W-130 - Impactor
Concentration (cm^{-3})

Height (km)	Size Range (μm)						
	>0.20	0.20-0.25	0.25-0.50	0.50-0.75	0.75-1.25	1.25-1.87	1.87-2.50
5.87	1.890	1.075	0.761	4.37×10^{-2}	9.27×10^{-3}	1.19×10^{-3}	-
6.20	0.962	0.552	0.377	2.66×10^{-2}	6.00×10^{-3}	-	-
6.53	0.915	0.482	0.391	3.11×10^{-2}	9.01×10^{-3}	1.50×10^{-3}	-
6.87	0.750	0.414	0.303	2.45×10^{-2}	7.45×10^{-3}	1.21×10^{-3}	-
7.20	0.823	0.473	0.330	2.99×10^{-2}	8.60×10^{-3}	1.44×10^{-3}	-
7.53	0.967	0.463	0.450	$3.94.10^{-2}$	1.27×10^{-2}	2.38×10^{-3}	-
7.87	0.815	0.391	0.385	2.95×10^{-2}	8.03×10^{-3}	1.25×10^{-3}	-
8.20	1.018	0.495	0.472	3.65×10^{-2}	1.22×10^{-2}	2.19×10^{-3}	-
8.53	0.872	0.367	0.431	4.70×10^{-2}	2.12×10^{-2}	4.55×10^{-3}	1.29×10^{-3}
8.87	0.858	0.373	0.389	6.30×10^{-2}	2.50×10^{-2}	6.42×10^{-3}	1.98×10^{-3}
9.20	1.008	0.325	0.500	9.96×10^{-2}	5.90×10^{-2}	1.79×10^{-2}	6.68×10^{-3}
9.53	0.598	0.268	0.281	3.33×10^{-2}	1.31×10^{-2}	3.06×10^{-3}	-
9.87	0.556	0.208	0.275	4.66×10^{-2}	1.93×10^{-2}	5.27×10^{-3}	1.69×10^{-3}
10.20	0.643	0.223	0.300	6.58×10^{-2}	3.54×10^{-2}	1.37×10^{-2}	5.35×10^{-3}
10.53	0.444	0.212	0.200	2.43×10^{-2}	6.57×10^{-3}	1.49×10^{-3}	-
10.87	0.793	0.300	0.398	6.07×10^{-2}	2.55×10^{-2}	6.94×10^{-3}	2.23×10^{-3}
11.20	0.601	0.336	0.249	1.32×10^{-2}	3.02×10^{-3}	-	-
11.53	0.862	0.341	0.394	7.23×10^{-2}	3.69×10^{-2}	1.34×10^{-2}	4.06×10^{-3}
11.87	0.440	0.225	0.191	1.87×10^{-2}	4.95×10^{-3}	-	-
12.20	0.582	0.256	0.260	4.31×10^{-2}	1.66×10^{-2}	4.81×10^{-3}	1.48×10^{-3}

W-130 - Impactor
Concentration (cm^{-3}) (Continued)

Height (km)	Size Range (μm)						
	>0.20	0.20-0.25	0.25-0.50	0.50-0.75	0.75-1.25	1.25-1.87	1.87-2.50
12.53	0.688	0.240	0.347	5.86×10^{-2}	2.97×10^{-2}	9.24×10^{-3}	3.26×10^{-3}
12.87	0.504	0.159	0.255	5.16×10^{-2}	2.81×10^{-2}	9.45×10^{-3}	3.55×10^{-3}
13.20	0.655	0.308	0.294	3.40×10^{-2}	1.49×10^{-2}	3.46×10^{-3}	1.00×10^{-3}
13.53	0.502	0.257	0.213	2.41×10^{-2}	6.83×10^{-3}	1.31×10^{-3}	-
13.87	0.585	0.224	0.296	4.18×10^{-2}	1.69×10^{-2}	5.14×10^{-3}	1.66×10^{-3}
14.20	0.509	0.261	0.221	2.13×10^{-2}	5.75×10^{-3}	-	-
14.53	0.644	0.340	0.275	2.17×10^{-2}	6.85×10^{-3}	-	-
14.87	1.054	0.389	0.537	7.35×10^{-2}	3.96×10^{-2}	1.15×10^{-2}	3.87×10^{-3}
15.20	0.971	0.355	0.495	6.65×10^{-2}	4.46×10^{-2}	1.06×10^{-2}	3.61×10^{-3}
15.53	0.875	0.340	0.409	7.55×10^{-2}	3.44×10^{-2}	1.20×10^{-2}	4.21×10^{-3}
15.87	0.514	0.186	0.264	4.00×10^{-2}	1.71×10^{-2}	5.55×10^{-3}	1.88×10^{-3}
16.20	0.187	0.652	0.958	1.56×10^{-2}	7.77×10^{-3}	2.56×10^{-3}	-
16.53	0.198	0.693	0.100	1.86×10^{-2}	8.35×10^{-3}	2.58×10^{-3}	-
16.87	0.257	0.910	0.130	2.00×10^{-2}	1.12×10^{-2}	3.48×10^{-3}	1.24×10^{-3}
17.20	0.361	0.129	0.184	2.75×10^{-2}	1.51×10^{-2}	3.85×10^{-3}	1.29×10^{-3}
17.53	0.420	0.159	0.198	3.90×10^{-2}	1.72×10^{-2}	5.16×10^{-3}	1.78×10^{-3}
17.87	0.459	0.175	0.231	3.28×10^{-2}	1.50×10^{-2}	4.06×10^{-3}	1.30×10^{-3}
18.20	0.483	0.194	0.220	4.25×10^{-2}	1.87×10^{-2}	5.53×10^{-3}	1.89×10^{-3}
18.53	0.590	0.218	0.299	4.41×10^{-2}	2.07×10^{-3}	6.55×10^{-3}	1.95×10^{-3}
18.87	0.522	0.241	0.256	4.26×10^{-2}	1.69×10^{-2}	4.46×10^{-3}	1.40×10^{-3}

W-130 - Impactor
Concentration (cm^{-3}) (Continued)

Height	Size Range (μm)						
	>0.20	0.20-0.25	0.25-0.50	0.50-0.75	0.75-1.25	1.25-1.87	1.87-2.50
19.20	0.588	0.266	0.264	3.54×10^{-3}	1.71×10^{-2}	4.42×10^{-3}	1.36×10^{-3}
19.53	0.650	0.256	0.312	4.88×10^{-2}	2.39×10^{-2}	7.07×10^{-3}	2.41×10^{-3}
19.87	0.558	0.232	0.257	4.13×10^{-2}	2.10×10^{-2}	5.22×10^{-3}	1.73×10^{-3}
20.20	0.501	0.194	0.240	3.95×10^{-2}	2.03×10^{-2}	5.70×10^{-3}	1.75×10^{-3}
20.53	0.470	0.181	0.235	3.30×10^{-2}	1.47×10^{-2}	5.80×10^{-3}	1.26×10^{-3}
20.87	0.389	0.175	0.174	2.55×10^{-2}	1.19×10^{-2}	2.79×10^{-3}	-
2120	0.319	0.124	0.162	2.08×10^{-2}	9.88×10^{-3}	2.28×10^{-3}	-
21.53	0.261	0.102	0.133	1.76×10^{-2}	6.46×10^{-3}	1.58×10^{-3}	-
2187	0.188	0.868	0.848	1.10×10^{-2}	4.42×10^{-3}	1.12×10^{-3}	-
22.20	0.133	0.560	0.672	8.00×10^{-3}	2.88×10^{-3}	-	-

W-130 - Filter Samples

Concentration ($\mu g/m^3$)

Height (km)	Element									
	Mg	Al	Ca	Ni	Cr	Cu	Pb	Mn	Fe	Zn
5.7 - 10.7	$\leq$0.3	$\leq$0.06	<0.3	<0.2	<0.02	0.02	<0.03	$\leq$0.004	<0.3	<0.6
10.7 - 15.0	<0.3	0.4	1.0	<0.2	$\leq$0.02	>0.7	0.04	0.5	0.6	<0.6
15.0 - 22.5	<0.3	0.06	<0.3	<0.2	<0.02	0.1	<0.03	$\leq$0.004	$\leq$0.3	<0.6

W-131

August 5, 1976

Laramie, Wyoming

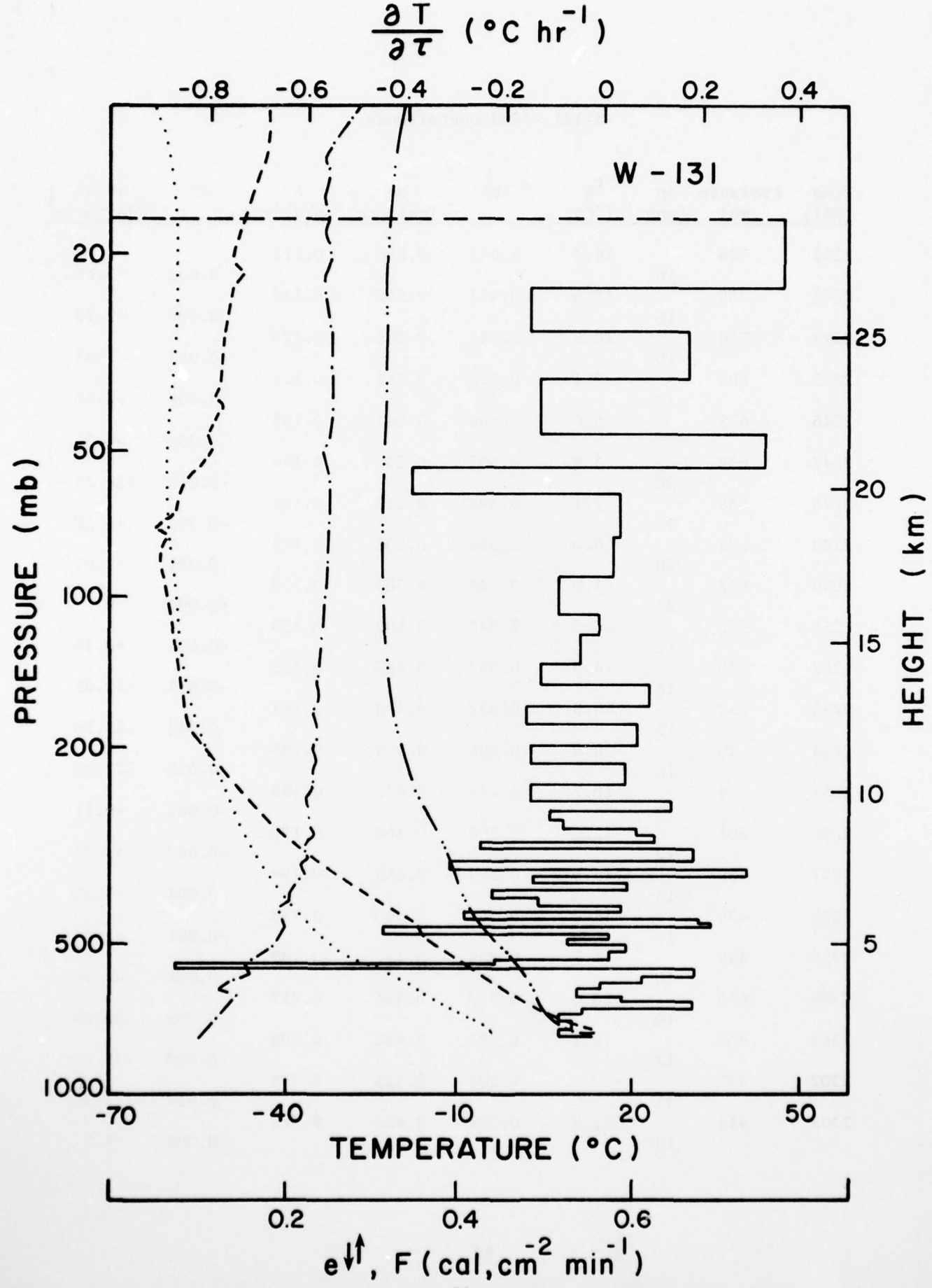
$\frac{\partial T}{\partial \tau}$ (°C hr^{-1})
-0.8
-0.6
-0.4
-0.2
0
0.2
0.4
W - 131
PRESSURE (mb)
20
50
100
200
500
1000
HEIGHT (km)
25
20
15
10
5
-70
-40
-10
20
50
TEMPERATURE (°C)
0.2
0.4
0.6
$e^{\downarrow\uparrow}$, F (cal, cm^{-2} min^{-1})

W-131 - Radiometersonde

Time (MST)	Pressure (mb)	Δp (mb)	t_b (°C)	e↓	e↑ (cal. cm^{-2} min^{-1})	F	ΔF	$\partial T/\partial \tau$ °C hr^{-1} x 10^2
2242	746		14.4	0.444	0.556	0.112		
		16					0.002	-3.06
2243	730		12.5	0.448	0.562	0.114		
		16					0.006	-9.19
2244	714		10.9	0.448	0.568	0.120		
		16					0.005	-7.64
2245	698		9.1	0.422	0.547	0.125		
		23					0.008	-8.50
2246	675		6.0	0.408	0.541	0.133		
		17					0.003	-4.31
2247	658		3.8	0.397	0.533	0.136		
		20					-0.015	+18.38
2248	638		2.1	0.394	0.515	0.121		
		16					-0.003	+4.59
2249	622		0.0	0.390	0.508	0.118		
		20					0.041	-5.02
2250	602		-1.9	0.344	0.503	0.159		
		20					+0.000	0
2251	582		-3.0	0.343	0.502	0.159		
		12					-0.004	+8.16
2252	570		-4.9	0.332	0.487	0.155		
		18					-0.014	+19.05
2253	552		-6.5	0.332	0.473	0.141		
		12					0.042	-85.75
2254	540		-9.0	0.296	0.479	0.183		
		16					0.015	-22.96
2255	524		-10.7	0.274	0.472	0.198		
		23					-0.002	+2.11
2256	501		-12.0	0.268	0.464	0.196		
		12					-0.002	+4.07
2257	489		-13.5	0.259	0.453	0.194		
		13					0.004	-7.53
2258	476		-15.0	0.252	0.450	0.198		
		17					-0.001	+1.44
2259	459		-15.7	0.238	0.437	0.199		
		10					0.008	-44.10
2300	449		-16.0	0.217	0.434	0.217		
		10					-0.009	+22.05
2301	439		-19.1	0.224	0.432	0.208		
		12					-0.010	+20.41
2302	427		-20.7	0.227	0.425	0.198		
		15					0.017	-27.76
2303	412		-21.9	0.209	0.424	0.215		
		10					-0.002	+4.9

W-131 - Radiometersonde (Continued)

Time (MST)	Pressure (mb)	Δp (mb)	t_b (°C)	e↓	e↑ (cal. cm^{-2} min^{-1})	F	ΔF	∂T/∂τ °C hr^{-1} x 10^2
2304	402		-23.4	0.206	0.419	0.213		
		14					0.007	-12.25
2305	388		-24.7	0.196	0.416	0.220		
		10					0.009	-22.05
2306	378		-26.3	0.190	0.419	0.229		
		11					-0.003	+6.66
2307	367		-28.2	0.186	0.412	0.226		
		14					0.008	-14.86
2308	353		-30.2	0.182	0.416	0.234		
		10					-0.012	+29.40
2309	343		-31.5	0.179	0.401	0.222		
		11					0.014	-31.16
2310	332		-33.4	0.166	0.402	0.236		
		15					-0.012	+19.6
2311	317		-37.1	0.176	0.400	0.224		
		9					0.009	-24.5
2312	308		-38.5	0.165	0.398	0.233		
		11					-0.005	+11.2
2313	297		-40.0	0.161	0.389	0.228		
		9					-0.003	+8.16
2314	288		-41.3	0.156	0.381	0.225		
		10					0.003	-7.35
2315	278		-43.6	0.154	0.382	0.228		
		15					0.006	-9.80
2316	263		-45.0	0.142	0.376	0.234		
		8					-0.005	+15.31
2317	255		-46.4	0.139	0.368	0.229		
2318	244		-47.7	0.130	0.364	0.234		
		20					0.012	-14.7
2319	235		-48.6	0.122	0.363	0.241		
2320	230		-49.8	0.120	0.358	0.238		
2321	217		-51.7	0.117	0.356	0.245		
		23					-0.006	+6.37
2322	212		-53.6	0.116	0.351	0.235		
2323	201		-55.5	0.114	0.351	0.237		
		17					0.010	-14.41
2324	195		-56.4	0.100	0.345	0.245		
2325	186		-56.4	0.100	0.340	0.240		
		18					-0.006	+8.16

W-131 - Radiometersonde (Continued)

Time (MST)	Pressure (mb)	Δp (mb)	t_b (°C)	e↓	e↑ (cal. cm^{-2} min^{-1})	F	ΔF	∂T/∂τ °C hr^{-1} x 10^2
2326	177		-56.7	0.099	0.338	0.239		
2327	171	13	-56.6	0.095	0.337	0.242	0.008	-15.07
2328	164		-56.3	0.088	0.335	0.247		
2329	156		-56.6	0.095	0.330	0.235		
2330	152	20	-57.0	0.093	0.334	0.241	-0.008	+9.8
2331	144		-58.2	0.091	0.330	0.239		
2332	139	10	-58.2	0.085	0.328	0.243	0.005	-12.25
2333	134		-58.4	0.081	0.325	0.244		
2334	127	18	-58.2	0.080	0.323	0.243	-0.03	-4.08
2335	116		-59.5	0.079	0.326	0.247		
2336	116	10	-59.1	0.078	0.325	0.247	0.0	0.0
2337	112		-59.7	0.078	0.325	0.247		
2338	106	17	-59.9	0.079	0.326	0.247	0.006	-8.64
2339	102		-59.9	0.078	0.326	0.248		
2340	97		-60.8	0.080	0.329	0.249		
2341	92		-62.2	0.074	0.328	0.254		
2342	89		-61.7	0.073	0.326	0.253		
2343	84		-61.7	0.070	0.327	0.256		
2344	81		-61.7	0.071	0.327	0.256		
2345	78	16	-60.0	0.067	0.322	0.255	-0.002	+3.06
2346	76		-61.1	0.069	0.325	0.256		
2347	73		-62.4	0.073	0.328	0.255		

W-131 - Radiometersonde (Continued)

Time (MST)	Pressure (mb)	Δp (mb)	t_b (°C)	e↓	e↑ (cal. cm^{-2}	F min^{-1})	ΔF	∂T/∂τ °C hr^{-1} x 10^2
2348	70		-59.8	0.067	0.322	0.255		
2349	68		-59.3	0.066	0.321	0.255		
2350	65		-58.9	0.066	0.321	0.255		
		13					-0.002	+3.76
2351	63		-59.0	0.066	0.323	0.257		
2352	60		-57.8	0.067	0.320	0.253		
2353	58		-56.6	0.064	0.319	0.255		
2354	56		-55.7	0.064	0.322	0.258		
		7					0.011	-38.50
2355	54		-55.5	0.062	0.325	0.263		
2356	53		-53.9	0.059	0.323	0.264		
2357	51		-53.1	0.067	0.320	0.253		
2358	49		-54.4	0.070	0.325	0.255		
		8					-0.011	+33.70
2359	47		-55.1	0.073	0.325	0.252		
0000	45		-54.7	0.072	0.072	0.253		
0001	44		-53.8	0.069	0.326	0.257		
0002	42		-52.3	0.065	0.322	0.257		
0003	41		-51.8	0.064	0.325	0.261		
		10					0.005	-12.25
0004	39		-52.3	0.068	0.326	0.258		
0005	39		-53.0	0.071	0.328	0.257		
0006	37		-51.8	0.067	0.324	0.257		
0007	35		-51.5	0.068	0.326	0.258		
0008	34		-51.4	0.071	0.325	0.254		
0009	33		-51.5	0.075	0.327	0.252		
0010	31		-47.8	0.067	0.319	0.252		
		7					-0.005	+17.5

W-131 - Radiometersonde (Continued)

Time (MST)	Pressure (mb)	Δp (mb)	t_b (°C)	e↓	e↑ (cal cm^{-2} min^{-1})	F	ΔF	∂T/∂τ °C hr^{-1} x 10^2
0011	30		-50.4	0.072	0.325	0.253		
0012	29		-50.4	0.072	0.325	0.253		
0013	28		-50.7	0.073	0.326	0.253		
0014	27		-49.7	0.071	0.325	0.254		
0015	25		-49.7	0.074	0.326	0.252		
0016	24	5	-49.5	0.074	0.326	0.252	0.003	-14.7
0017	23		-47.8	0.069	0.325	0.256		
0018	22		-47.3	0.073	0.324	0.251		
0019	22		-47.9	0.075	0.325	0.250		
0020	21		-48.5	0.075	0.326	0.251		
0021	20	6	-48.6	0.070	0.324	0.254	-0.009	+36.75
0022	19		-48.6	0.076	0.323	0.247		
0023	18		-47.2	0.072	0.322	0.250		
0024	17		-46.4	0.072	0.321	0.249		
0025	17		-45.9	0.073	0.320	0.247		
0026	16		-46.2	0.073	0.324	0.251		
0027	15		-46.4	0.074	0.326	0.252		
0028	15		-45.7	0.070	0.325	0.255		
0029	15		-44.8	0.069	0.324	0.255		
0030	13	7	-43.7	0.073	0.321	0.248	0.045	-157.50
0031	13		-43.0	0.069	0.327	0.258		
0032	12		-43.1	0.069	0.327	0.258		

W-131 - Radiometersonde (Continued)

Time (MST)	Pressure (mb)	Δp (mb)	t_b (°C)	e↓	e↑ (cal cm^{-2} min^{-1})	F	ΔF	$\partial T/\partial \tau$ °C hr^{-1} x 10^2
0033	12		-43.1	0.072	0.326	0.254		
0034	11		-43.2	0.060	0.329	0.269		
0035	11		-43.5	0.048	0.335	0.287		
0036	10		-43.5	0.047	0.339	0.292		

W-132

August 6, 1976

Laramie, Wyoming

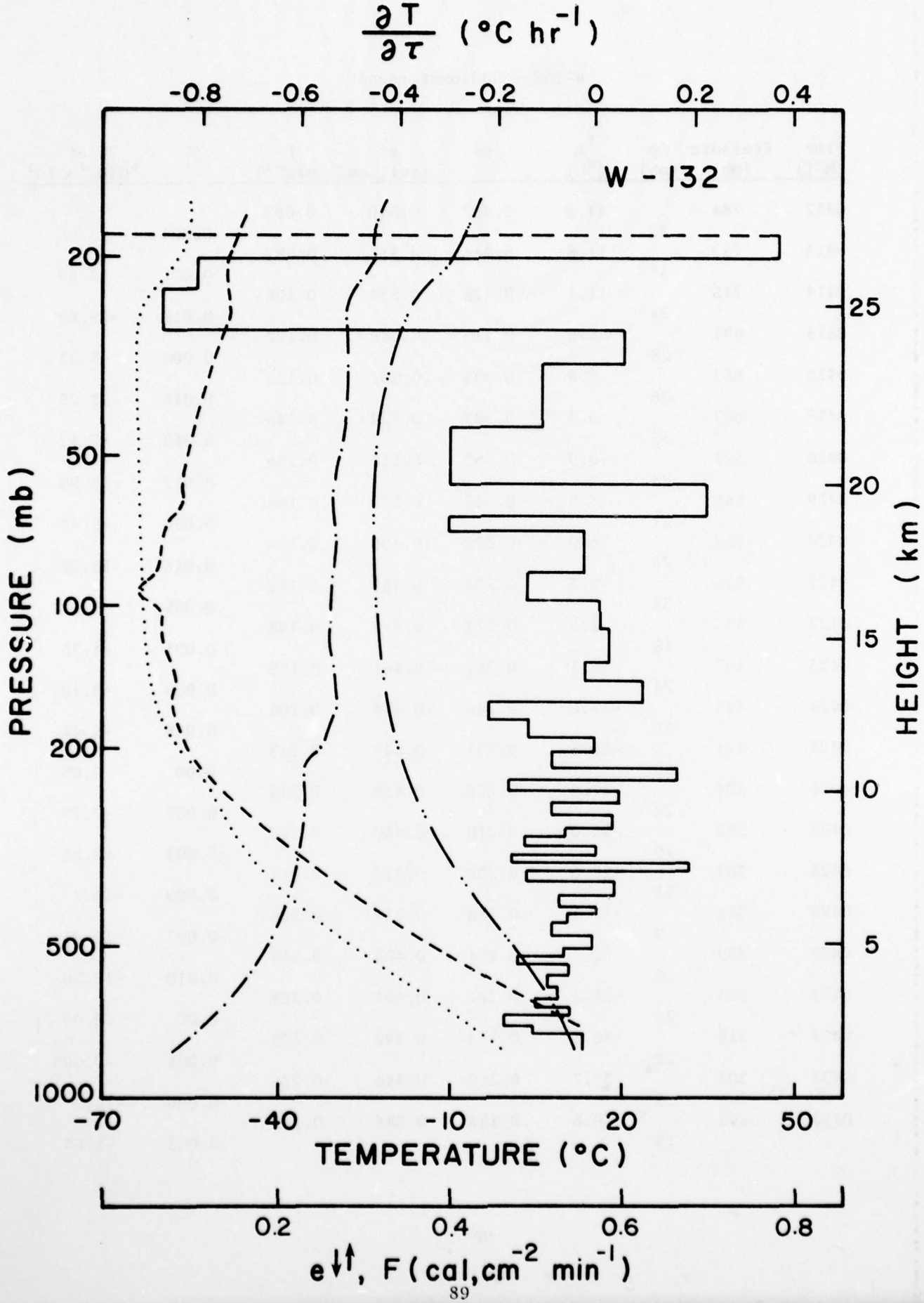
$\frac{\partial T}{\partial \tau}$ (°C hr^{-1})
-0.8
-0.6
-0.4
-0.2
0
0.2
0.4
W - 132
PRESSURE (mb)
20
50
100
200
500
1000
HEIGHT (km)
25
20
15
10
5
-70
-40
-10
20
50
TEMPERATURE (°C)
0.2
0.4
0.6
0.8
$e^{\downarrow\uparrow}$, F (cal, cm^{-2} min^{-1})

W-132 - Radiometersonde

Time (MST)	Pressure (mb)	Δp (mb)	t_b (°C)	e↓	e↑ (cal. cm^{-2} min^{-1})	F	ΔF	$\partial T/\partial \tau$ °C hr^{-1} x 10^2
0412	784		11.2	0.457	0.540	0.083		
		32					0.004	-3.06
0413	752		11.8	0.446	0.533	0.087		
		37					0.021	-13.89
0414	715		11.1	0.426	0.534	0.108		
		24					0.019	-19.69
0415	681		8.9	0.413	0.540	0.127		
		28					0.006	-5.24
0416	653		6.5	0.398	0.531	0.133		
		26					0.013	-12.25
0417	627		3.4	0.383	0.529	0.146		
		33					0.010	-7.42
0418	594		-0.9	0.363	0.519	0.156		
		28					0.012	-10.50
0419	566		-3.8	0.342	0.510	0.168		
		27					0.006	-5.44
0420	539		-6.9	0.322	0.496	0.174		
		23					0.015	-15.97
0421	516		-9.3	0.294	0.483	0.189		
		31					0.009	-7.11
0422	485		-12.5	0.274	0.472	0.198		
		18					0.001	-1.35
0423	467		-15.1	0.262	0.461	0.199		
		24					0.009	-9.19
0424	443		-17.6	0.246	0.454	0.208		
		19					0.005	-6.44
0425	424		-20.5	0.231	0.444	0.213		
		20					0.00	0.00
0426	404		-22.9	0.226	0.439	0.213		
		22					0.007	-7.79
0427	382		-26.0	0.210	0.430	0.220		
		19					-0.003	+3.85
0428	363		-28.6	0.200	0.417	0.217		
		15					0.009	-14.7
0429	348		-30.6	0.188	0.414	0.226		
		9					-0.007	+19.05
0430	339		-32.3	0.184	0.403	0.219		
		14					0.010	-17.50
0431	325		-34.3	0.172	0.401	0.229		
		22					0.00	0.00
0432	315		-36.3	0.163	0.392	0.229		
		22					0.003	-0.003
0433	303		-37.7	0.160	0.386	0.226		
		10					0.006	-14.7
0434	293		-39.6	0.153	0.385	0.232		
		13					0.003	-5.64

W-132 - Radiometersonde (Continued)

Time (MST)	Pressure (mb)	Δp (mb)	t_b (°C)	e↓	e↑ (cal. cm^{-2} min^{-1})	F	ΔF	$\partial T/\partial \tau$ °C hr^{-1} x 10^2
0435	280		-49.9	0.144	0.379	0.235		
		17					-0.003	+4.31
0436	272		-43.8	0.143	0.375	0.232		
0437	263		-44.8	0.137	0.369	0.232		
		10					0.004	-9.86
0438	253		-46.8	0.133	0.369	0.236		
		18					-0.004	+5.44
0439	246		-48.2	0.128	0.362	0.234		
0440	235		-49.6	0.124	0.356	0.232		
		7					0.005	-17.50
0441	228		-50.7	0.116	0.353	0.237		
		15					-0.010	+16.33
0442	220		-51.8	0.114	0.346	0.232		
0443	213		-52.5	0.112	0.339	0.227		
		16					0.006	-9.19
0444	205		-54.0	0.107	0.340	0.233		
0445	197		-54.7	0.093	0.336	0.243		
		14					0.012	-0.21
0446	191		-55.0	0.086	0.336	0.250		
0447	183		-56.2	0.081	0.336	0.255		
		13					0.007	-13.19
0448	177		-56.4	0.073	0.336	0.263		
0449	170		-57.2	0.071	0.333	0.262		
		13					0.012	-22.61
0450	165		-57.5	0.068	0.333	0.265		
0451	157		-58.1	0.059	0.333	0.274		
		15					-0.006	+9.8
0452	152		-57.8	0.058	0.330	0.272		
0453	146		-58.0	0.058	0.326	0.268		
0454	142		-57.2	0.056	0.324	0.268		
		12					0.001	-2.04
0455	136		-57.8	0.055	0.324	0.269		
0456	130		-58.4	0.055	0.324	0.269		
0457	125		-58.9	0.055	0.321	0.266		
		19					-0.002	+2.57

W-132 - Radiometersonde (Continued)

Time (MST)	Pressure (mb)	Δp (mb)	t_b (°C)	e↓	e↑	F (cal. cm^{-2} min^{-1})	ΔF	∂T/∂τ °C hr^{-1} x 10^2
0458	120		-59.5	0.055	0.321	0.266		
0459	115		-59.3	0.054	0.321	0.267		
0500	111		-59.5	0.054	0.321	0.267		
0501	105		-59.5	0.054	0.320	0.266		
		14					-0.001	+1.74
0502	102		-59.7	0.052	0.320	0.268		
0503	97		-62.7	0.054	0.320	0.266		
0504	93		-62.4	0.052	0.321	0.269		
		14					0.008	-14.00
0505	89		-61.5	0.048	0.321	0.273		
0506	86		-61.0	0.047	0.319	0.272		
0507	83		-59.5	0.044	0.318	0.274		
0508	79		-59.6	0.044	0.319	0.275		
		13					0.001	-1.86
0509	77		-60.5	0.046	0.319	0.273		
0510	74		-59.3	0.044	0.319	0.275		
0511	70		-59.3	0.047	0.322	0.275		
		4					0.005	-30.62
0512	68		-59.1	0.046	0.323	0.277		
0513	66		-57.6	0.040	0.320	0.280		
0514	63		-56.6	0.040	0.317	0.277		
		10					-0.009	+22.05
0515	61		-56.1	0.044	0.315	0.271		
0516	53		-56.1	0.045	0.318	0.273		
0517	56		-56.3	0.049	0.320	0.271		
0518	54		-56.1	0.050	0.322	0.272		
0519	52		-56.0	0.048	0.322	0.274		
		13					0.016	-30.15
0520	50		-54.6	0.043	0.319	0.276		
0521	48		-52.2	0.038	0.317	0.279		

W-132 - Radiometersonde (Continued)

Time (MST)	Pressure (mb)	Δp (mb)	t_b (°C)	e↓	e↑ (cal. cm^{-2} min^{-1})	F	ΔF	∂T/∂τ °C hr^{-1} x 10^2
0522	46		-52.8	0.040	0.332	0.282		
0523	44		-54.0	0.042	0.327	0.285		
0524	43		-53.4	0.041	0.328	0.287		
0525	41		-52.4	0.039	0.325	0.286		
0526	39		-51.9	0.038	0.327	0.289		
		11					0.005	-11.13
0527	38		-51.2	0.042	0.327	0.285		
0528	37		-50.6	0.038	0.329	0.291		
0529	35		-49.9	0.038	0.329	0.291		
0530	34		-49.9	0.040	0.330	0.290		
0531	33		-48.7	0.037	0.330	0.293		
0532	32		-49.7	0.041	0.333	0.292		
0533	30		-49.7	0.043	0.335	0.292		
		4					-0.001	+6.12
0534	30		-48.4	0.048	0.336	0.288		
0535	28		-48.6	0.050	0.341	0.291		
0536	28		-48.6	0.050	0.345	0.295		
0537	27		-48.6	0.050	0.348	0.298		
		5					0.018	-88.20
0538	26		-47.7	0.053	0.348	0.295		
0539	25		-47.6	0.054	0.349	0.295		
0540	24		-47.0	0.062	0.359	0.297		
0541	23		-46.7	0.067	0.376	0.309		
0542	22		-46.9	0.092	0.381	0.289		
		3					0.010	-81.66
0543	22		-47.1	0.091	0.393	0.302		
0544	21		-47.7	0.097	0.407	0.310		
0545	20		-47.2	0.095	0.414	0.319		

AD-A060 383 WYOMING UNIV LARAMIE DEPT OF PHYSICS AND ASTRONOMY F/G 7/4
UNIVERSITY OF WYOMING/LENINGRAD STATE UNIVERSITY COOPERATIVE ST--ETC(U)
JUL 78 J M ROSEN, D J HOFMANN DOT-FAA76WA-3782

UNCLASSIFIED FAA-AEQ-78-22 NL

2 OF 2
AD
A060 383

END
DATE
FILMED
1-79
DDC

W-132 - Radiometersonde (Continued)

Time (MST)	Pressure (mb)	Δp (mb)	t_b (°C)	e↓	e↑	F (cal. cm^{-2} min^{-1})	ΔF	$\partial T/\partial \tau$ °C hr^{-1} x 10^2
0546	20	2	-47.7	0.105	0.417	0.312	-0.008	+38.00
0547	19		-47.4	0.115	0.417	0.302		
0548	18		-47.0	0.112	0.425	0.313		
0549	18	2	-45.8	0.110	0.421	0.311	0.016	-196.0
0550	17		-44.4	0.111	0.425	0.314		
0551	16		-44.1	0.111	0.438	0.327		

W-133

August 6, 1976

Laramie, Wyoming

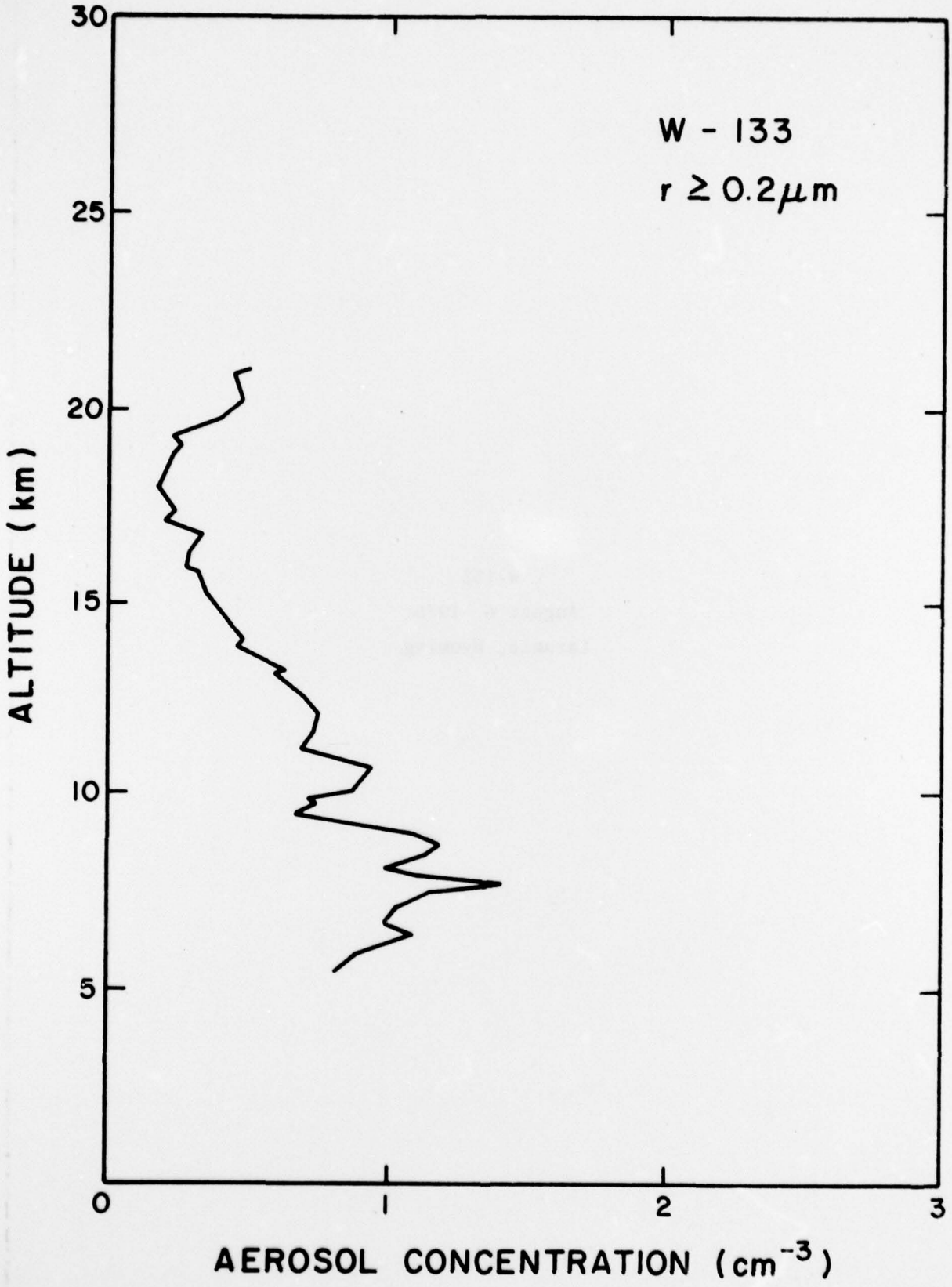
W - 133
r ≥ 0.2μm
ALTITUDE (km)
30
25
20
15
10
5
0
1
2
3
AEROSOL CONCENTRATION (cm⁻³)

W-133 - Impactor
Concentration (cm^{-3})

Height (km)	Size Range (μm)						
	>0.20	0.20-0.25	0.25-0.50	0.50-0.75	0.75-1.25	1.25-1.87	1.87-2.50
5.57	0.835	0.473	0.341	1.69×10^{-2}	3.70×10^{-3}	-	-
5.90	0.828	0.414	0.372	3.18×10^{-2}	8.39×10^{-3}	1.36×10^{-3}	-
6.23	1.010	0.501	0.436	5.27×10^{-2}	1.67×10^{-2}	3.48×10^{-3}	-
6.57	1.151	0.433	0.580	8.87×10^{-2}	3.63×10^{-2}	1.00×10^{-2}	3.20×10^{-3}
6.90	0.950	0.386	0.461	6.99×10^{-2}	2.54×10^{-2}	6.21×10^{-3}	1.82×10^{-3}
7.23	0.962	0.411	0.473	5.10×10^{-2}	2.13×10^{-2}	4.71×10^{-3}	1.29×10^{-3}
7.57	1.252	0.568	0.584	6.68×10^{-2}	2.55×10^{-2}	5.81×10^{-3}	1.62×10^{-3}
7.90	1.418	0.507	0.675	0.145	6.36×10^{-2}	1.99×10^{-3}	7.08×10^{-3}
8.23	1.017	0.382	0.515	7.40×10^{-2}	3.39×10^{-2}	9.40×10^{-3}	3.03×10^{-3}
8.57	1.063	0.382	0.480	0.117	5.80×10^{-2}	1.91×10^{-2}	7.20×10^{-3}
8.90	1.118	0.468	0.502	8.87×10^{-2}	4.42×10^{-2}	1.11×10^{-2}	3.58×10^{-3}
9.23	1.115	0.486	0.512	7.05×10^{-2}	3.47×10^{-2}	9.34×10^{-3}	2.96×10^{-3}
9.57	0.628	0.215	0.315	6.02×10^{-2}	2.70×10^{-2}	8.05×10^{-3}	2.75×10^{-3}
9.90	0.815	0.332	0.397	5.43×10^{-2}	2.38×10^{-2}	6.39×10^{-3}	2.01×10^{-3}
10.23	0.710	0.416	0.265	2.27×10^{-2}	6.18×10^{-3}	-	-
10.57	0.910	0.372	0.451	5.58×10^{-2}	2.09×10^{-3}	5.55×10^{-3}	1.66×10^{-3}
10.90	0.987	0.396	0.485	7.38×10^{-2}	2.88×10^{-2}	7.46×10^{-3}	2.31×10^{-3}
11.23	0.867	0.420	0.400	3.43×10^{-2}	9.75×10^{-3}	1.72×10^{-3}	-
11.57	0.708	0.386	0.301	1.66×10^{-2}	3.97×10^{-3}	-	-
11.90	0.757	0.366	0.350	2.93×10^{-2}	1.00×10^{-2}	1.62×10^{-3}	-

W-133 - Impactor
Concentration (cm^{-3}) (Continued)

Height (km)	Size Range (μm)						
	>0.20	0.20-0.25	0.25-0.50	0.50-0.75	0.75-1.25	1.25-1.87	1.87-2.50
12.23	0.777	0.315	0.395	5.15×10^{-2}	1.90×10^{-2}	4.70×10^{-3}	1.38×10^{-3}
12.57	0.745	0.327	0.345	4.84×10^{-2}	1.95×10^{-2}	4.00×10^{-3}	1.15×10^{-3}
12.90	0.693	0.251	0.351	5.60×10^{-2}	2.45×10^{-2}	8.15×10^{-3}	2.78×10^{-3}
13.23	0.548	0.233	0.244	4.29×10^{-2}	2.11×10^{-2}	5.19×10^{-3}	1.65×10^{-3}
13.57	0.679	0.238	0.342	5.69×10^{-2}	2.89×10^{-2}	9.70×10^{-3}	3.10×10^{-3}
13.90	0.442	0.178	0.210	3.50×10^{-2}	1.41×10^{-2}	3.73×10^{-3}	1.19×10^{-3}
14.23	0.477	0.178	0.229	4.35×10^{-2}	1.92×10^{-2}	6.33×10^{-3}	1.95×10^{-3}
14.57	0.467	0.173	0.236	3.62×10^{-2}	1.52×10^{-2}	4.99×10^{-3}	1.68×10^{-3}
14.90	0.404	0.147	0.206	3.15×10^{-2}	1.50×10^{-2}	3.85×10^{-3}	1.46×10^{-3}
15.23	0.385	0.143	0.195	2.88×10^{-2}	1.36×10^{-2}	3.44×10^{-3}	1.28×10^{-3}
15.57	0.324	0.133	0.144	2.97×10^{-2}	1.26×10^{-2}	3.56×10^{-3}	1.18×10^{-3}
15.90	0.299	0.118	0.142	2.49×10^{-2}	1.14×10^{-2}	2.89×10^{-3}	-
16.23	0.282	0.107	0.141	2.18×10^{-2}	1.12×10^{-2}	2.87×10^{-3}	-
16.57	0.291	0.116	0.135	2.36×10^{-2}	1.24×10^{-2}	3.39×10^{-3}	1.16×10^{-3}
16.90	0.334	0.129	0.158	2.63×10^{-2}	1.48×10^{-2}	4.62×10^{-3}	1.63×10^{-3}
17.27	0.181	0.659	0.882	1.73×10^{-2}	8.78×10^{-3}	2.62×10^{-3}	-
17.57	0.234	0.930	0.108	2.09×10^{-2}	9.39×10^{-3}	2.72×10^{-3}	-
17.90	0.183	0.675	0.925	1.45×10^{-2}	6.86×10^{-3}	2.00×10^{-3}	-
18.23	0.178	0.662	0.890	1.46×10^{-2}	6.05×10^{-3}	2.19×10^{-3}	-
18.57	0.198	0.953	0.915	1.40×10^{-2}	5.66×10^{-3}	2.24×10^{-3}	-

W-133 - Impactor
Concentration (cm^{-3}) (Continued)

Height (km)	Size Range (μm)						
	>0.20	0.20-0.25	0.25-0.50	0.50-0.75	0.75-1.25	1.25-1.87	1.87-2.50
18.90	0.230	0.101	0.106	1.52×10^{-2}	7.16×10^{-3}	1.67×10^{-3}	-
19.23	0.267	0.106	0.132	1.98×10^{-2}	7.61×10^{-3}	1.94×10^{-3}	-
19.57	0.232	0.860	0.116	1.93×10^{-2}	8.12×10^{-3}	2.29×10^{-3}	-
19.90	0.425	0.158	0.214	3.16×10^{-2}	1.59×10^{-2}	4.20×10^{-3}	1.40×10^{-3}
20.23	0.428	0.178	0.192	3.24×10^{-2}	1.45×10^{-2}	5.69×10^{-3}	1.24×10^{-3}
20.57	0.481	0.192	0.239	3.21×10^{-2}	1.37×10^{-2}	3.82×10^{-3}	1.08×10^{-3}
20.90	0.454	0.205	0.206	2.81×10^{-2}	1.16×10^{-2}	3.18×10^{-3}	-
21.23	0.485	0.201	0.236	3.10×10^{-2}	1.33×10^{-2}	2.92×10^{-3}	-

W-133 - Filter Samples

Concentration ($\mu g/m^3$)

Height (km)	Element									
	Mg	Al	Ca	Ni	Cr	Cu	Pb	Mn	Fe	Zn
5.4 - 10.4	$\leq$0.3	0.06	3.3	<0.2	$\leq$0.02	>0.7	$\leq$0.03	$\leq$0.004	$\leq$0.3	<0.6
10.4 - 14.75	<0.3	0.2	0.5	<0.2	$\leq$0.02	0.05	<0.03	0.01	<0.3	<0.6
14.75 - 21.5	<0.3	0.2	0.4	$\leq$0.2	<0.02	0.05	<0.03	0.01	$\leq$0.3	<0.6